2

Kinematics

A *manipulator* can be schematically represented from a mechanical viewpoint as a kinematic chain of rigid bodies (*links*) connected by means of revolute or prismatic *joints*. One end of the chain is constrained to a base, while an *end-effector* is mounted to the other end. The resulting motion of the structure is obtained by composition of the elementary motions of each link with respect to the previous one. Therefore, in order to manipulate an object in space, it is necessary to describe the end-effector position and orientation. This chapter is dedicated to the derivation of the *direct kinematics equation* through a systematic, general approach based on linear algebra. This allows the end-effector position and orientation (*pose*) to be expressed as a function of the joint variables of the mechanical structure with respect to a reference frame. Both open-chain and closed-chain kinematic structures are considered. With reference to a *minimal representation of orientation*, the concept of *operational space* is introduced and its relationship with the *joint space* is established. Furthermore, a *calibration* technique of the manipulator kinematic parameters is presented. The chapter ends with the derivation of solutions to the *inverse kinematics problem*, which consists of the determination of the joint variables corresponding to a given end-effector pose.

2.1 Pose of a Rigid Body

A *rigid body* is completely described in space by its *position* and *orientation* (in brief *pose*) with respect to a reference frame. As shown in Fig. 2.1, let O–xyz be the orthonormal reference frame and $\boldsymbol{x}$, $\boldsymbol{y}$, $\boldsymbol{z}$ be the unit vectors of the frame axes.

The position of a point O' on the rigid body with respect to the coordinate frame O–xyz is expressed by the relation

$$\boldsymbol{o}' = o'_x \boldsymbol{x} + o'_y \boldsymbol{y} + o'_z \boldsymbol{z},$$

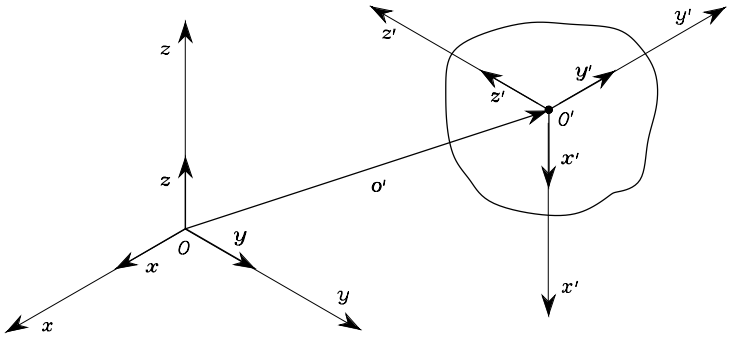

Fig. 2.1. Position and orientation of a rigid body

where o'_x, o'_y, o'_z denote the components of the vector $\boldsymbol{o}' \in \mathbb{R}^3$ along the frame axes; the position of O' can be compactly written as the (3×1) vector

$$\boldsymbol{o}' = \begin{bmatrix} o'_x \\ o'_y \\ o'_z \end{bmatrix}. \tag{2.1}$$

Vector $\boldsymbol{o}'$ is a bound vector since its line of application and point of application are both prescribed, in addition to its direction and norm.

In order to describe the rigid body orientation, it is convenient to consider an orthonormal frame attached to the body and express its unit vectors with respect to the reference frame. Let then O'–$x'y'z'$ be such a frame with origin in O' and $\boldsymbol{x}'$, $\boldsymbol{y}'$, $\boldsymbol{z}'$ be the unit vectors of the frame axes. These vectors are expressed with respect to the reference frame O–xyz by the equations:

$$\begin{aligned} \boldsymbol{x}' &= x'_x\boldsymbol{x} + x'_y\boldsymbol{y} + x'_z\boldsymbol{z} \\ \boldsymbol{y}' &= y'_x\boldsymbol{x} + y'_y\boldsymbol{y} + y'_z\boldsymbol{z} \\ \boldsymbol{z}' &= z'_x\boldsymbol{x} + z'_y\boldsymbol{y} + z'_z\boldsymbol{z}. \end{aligned} \tag{2.2}$$

The components of each unit vector are the direction cosines of the axes of frame O'–$x'y'z'$ with respect to the reference frame O–xyz.

2.2 Rotation Matrix

By adopting a compact notation, the three unit vectors in (2.2) describing the body orientation with respect to the reference frame can be combined in the (3×3) matrix

$$\boldsymbol{R} = \begin{bmatrix} \boldsymbol{x}' & \boldsymbol{y}' & \boldsymbol{z}' \end{bmatrix} = \begin{bmatrix} x'_x & y'_x & z'_x \\ x'_y & y'_y & z'_y \\ x'_z & y'_z & z'_z \end{bmatrix} = \begin{bmatrix} \boldsymbol{x}'^T\boldsymbol{x} & \boldsymbol{y}'^T\boldsymbol{x} & \boldsymbol{z}'^T\boldsymbol{x} \\ \boldsymbol{x}'^T\boldsymbol{y} & \boldsymbol{y}'^T\boldsymbol{y} & \boldsymbol{z}'^T\boldsymbol{y} \\ \boldsymbol{x}'^T\boldsymbol{z} & \boldsymbol{y}'^T\boldsymbol{z} & \boldsymbol{z}'^T\boldsymbol{z} \end{bmatrix}, \tag{2.3}$$

which is termed *rotation matrix*.

It is worth noting that the column vectors of matrix $\boldsymbol{R}$ are mutually orthogonal since they represent the unit vectors of an orthonormal frame, i.e.,

$$\boldsymbol{x}'^T\boldsymbol{y}' = 0 \qquad \boldsymbol{y}'^T\boldsymbol{z}' = 0 \qquad \boldsymbol{z}'^T\boldsymbol{x}' = 0.$$

Also, they have unit norm

$$\boldsymbol{x}'^T\boldsymbol{x}' = 1 \qquad \boldsymbol{y}'^T\boldsymbol{y}' = 1 \qquad \boldsymbol{z}'^T\boldsymbol{z}' = 1.$$

As a consequence, $\boldsymbol{R}$ is an *orthogonal* matrix meaning that

$$\boldsymbol{R}^T\boldsymbol{R} = \boldsymbol{I}_3 \tag{2.4}$$

where $\boldsymbol{I}_3$ denotes the (3×3) identity matrix.

If both sides of (2.4) are postmultiplied by the inverse matrix $\boldsymbol{R}^{-1}$, the useful result is obtained:

$$\boldsymbol{R}^T = \boldsymbol{R}^{-1}, \tag{2.5}$$

that is, the transpose of the rotation matrix is equal to its inverse. Further, observe that $\det(\boldsymbol{R}) = 1$ if the frame is right-handed, while $\det(\boldsymbol{R}) = -1$ if the frame is left-handed.

The above-defined rotation matrix belongs to the *special orthonormal group* $SO(m)$ of the real $(m \times m)$ matrices with othonormal columns and determinant equal to 1; in the case of spatial rotations it is $m = 3$, whereas in the case of planar rotations it is $m = 2$.

2.2.1 Elementary Rotations

Consider the frames that can be obtained via *elementary rotations* of the reference frame about one of the coordinate axes. These rotations are positive if they are made counter-clockwise about the relative axis.

Suppose that the reference frame O–xyz is rotated by an angle α about axis z (Fig. 2.2), and let O–$x'y'z'$ be the rotated frame. The unit vectors of the new frame can be described in terms of their components with respect to the reference frame. Consider the frames that can be obtained via *elementary rotations* of the reference frame about one of the coordinate axes. These rotations are positive if they are made counter-clockwise about the relative axis.

Suppose that the reference frame O–xyz is rotated by an angle α about axis z (Fig. 2.2), and let O–$x'y'z'$ be the rotated frame. The unit vectors of the new frame can be described in terms of their components with respect to the reference frame, i.e.,

$$\boldsymbol{x}' = \begin{bmatrix} \cos\alpha \\ \sin\alpha \\ 0 \end{bmatrix} \qquad \boldsymbol{y}' = \begin{bmatrix} -\sin\alpha \\ \cos\alpha \\ 0 \end{bmatrix} \qquad \boldsymbol{z}' = \begin{bmatrix} 0 \\ 0 \\ 1 \end{bmatrix}.$$

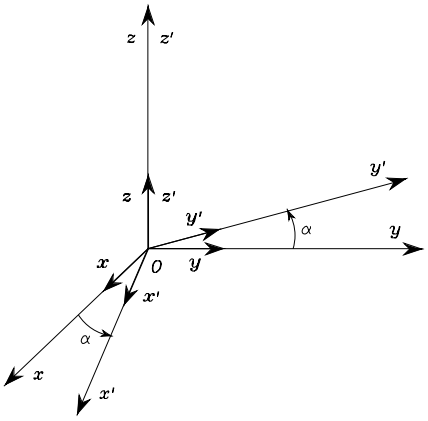

Fig. 2.2. Rotation of frame O–xyz by an angle α about axis z

Hence, the rotation matrix of frame O–$x'y'z'$ with respect to frame O–xyz is

$$\boldsymbol{R}_z(\alpha) = \begin{bmatrix} \cos\alpha & -\sin\alpha & 0 \\ \sin\alpha & \cos\alpha & 0 \\ 0 & 0 & 1 \end{bmatrix}. \tag{2.6}$$

In a similar manner, it can be shown that the rotations by an angle β about axis y and by an angle γ about axis x are respectively given by

$$\boldsymbol{R}_y(\beta) = \begin{bmatrix} \cos\beta & 0 & \sin\beta \\ 0 & 1 & 0 \\ -\sin\beta & 0 & \cos\beta \end{bmatrix} \tag{2.7}$$

$$\boldsymbol{R}_x(\gamma) = \begin{bmatrix} 1 & 0 & 0 \\ 0 & \cos\gamma & -\sin\gamma \\ 0 & \sin\gamma & \cos\gamma \end{bmatrix}. \tag{2.8}$$

These matrices will be useful to describe rotations about an arbitrary axis in space.

It is easy to verify that for the elementary rotation matrices in (2.6)–(2.8) the following property holds:

$$\boldsymbol{R}_k(-\vartheta) = \boldsymbol{R}_k^T(\vartheta) \qquad\qquad k = x, y, z. \tag{2.9}$$

In view of (2.6)–(2.8), the rotation matrix can be attributed a geometrical meaning; namely, the matrix $\boldsymbol{R}$ describes the rotation about an axis in space needed to align the axes of the reference frame with the corresponding axes of the body frame.

2.2.2 Representation of a Vector

In order to understand a further geometrical meaning of a rotation matrix, consider the case when the origin of the body frame coincides with the origin

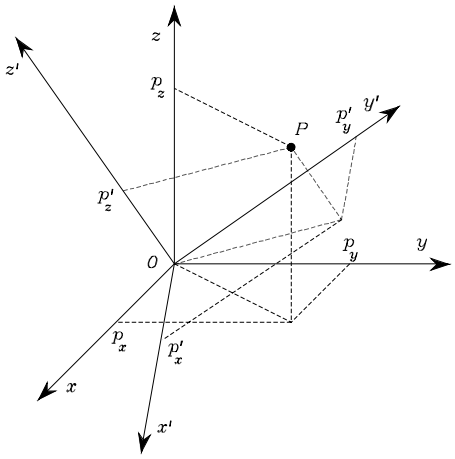

Fig. 2.3. Representation of a point P in two different coordinate frames

of the reference frame (Fig. 2.3); it follows that $\boldsymbol{o}' = \mathbf{0}$, where $\mathbf{0}$ denotes the (3×1) null vector. A point P in space can be represented either as

$$\boldsymbol{p} = \begin{bmatrix} p_x \\ p_y \\ p_z \end{bmatrix}$$

with respect to frame O–xyz, or as

$$\boldsymbol{p}' = \begin{bmatrix} p'_x \\ p'_y \\ p'_z \end{bmatrix}$$

with respect to frame O–$x'y'z'$.

Since $\boldsymbol{p}$ and $\boldsymbol{p}'$ are representations of the same point P, it is

$$\boldsymbol{p} = p'_x \boldsymbol{x}' + p'_y \boldsymbol{y}' + p'_z \boldsymbol{z}' = \begin{bmatrix} \boldsymbol{x}' & \boldsymbol{y}' & \boldsymbol{z}' \end{bmatrix} \boldsymbol{p}'$$

and, accounting for (2.3), it is

$$\boldsymbol{p} = \boldsymbol{R}\boldsymbol{p}'. \tag{2.10}$$

The rotation matrix $\boldsymbol{R}$ represents the *transformation matrix* of the vector coordinates in frame O–$x'y'z'$ into the coordinates of the same vector in frame O–xyz. In view of the orthogonality property (2.4), the inverse transformation is simply given by

$$\boldsymbol{p}' = \boldsymbol{R}^T \boldsymbol{p}. \tag{2.11}$$

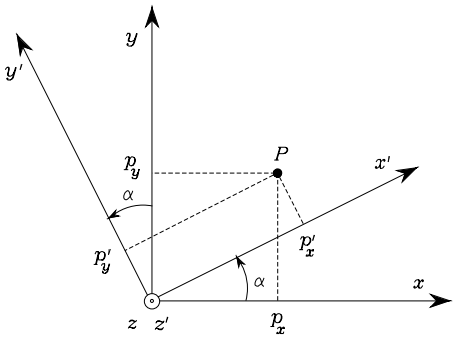

Fig. 2.4. Representation of a point P in rotated frames

Example 2.1

Consider two frames with common origin mutually rotated by an angle α about the axis z. Let $\boldsymbol{p}$ and $\boldsymbol{p}'$ be the vectors of the coordinates of a point P, expressed in the frames O–xyz and O–$x'y'z'$, respectively (Fig. 2.4). On the basis of simple geometry, the relationship between the coordinates of P in the two frames is

$$\begin{aligned} p_x &= p'_x \cos\alpha - p'_y \sin\alpha \\ p_y &= p'_x \sin\alpha + p'_y \cos\alpha \\ p_z &= p'_z. \end{aligned}$$

Therefore, the matrix (2.6) represents not only the orientation of a frame with respect to another frame, but it also describes the transformation of a vector from a frame to another frame with the same origin.

2.2.3 Rotation of a Vector

A rotation matrix can be also interpreted as the matrix operator allowing rotation of a vector by a given angle about an arbitrary axis in space. In fact, let $\boldsymbol{p}'$ be a vector in the reference frame O–xyz; in view of orthogonality of the matrix $\boldsymbol{R}$, the product $\boldsymbol{R}\boldsymbol{p}'$ yields a vector $\boldsymbol{p}$ with the same norm as that of $\boldsymbol{p}'$ but rotated with respect to $\boldsymbol{p}'$ according to the matrix $\boldsymbol{R}$. The norm equality can be proved by observing that $\boldsymbol{p}^T\boldsymbol{p} = \boldsymbol{p}'^T\boldsymbol{R}^T\boldsymbol{R}\boldsymbol{p}'$ and applying (2.4). This interpretation of the rotation matrix will be revisited later.

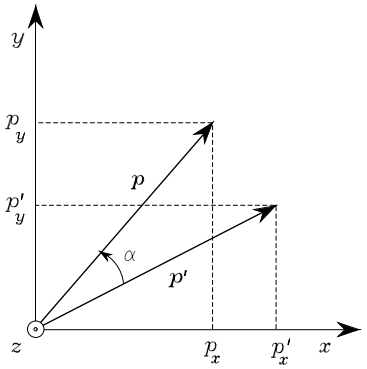

Fig. 2.5. Rotation of a vector

Example 2.2

Consider the vector $\boldsymbol{p}$ which is obtained by rotating a vector $\boldsymbol{p}'$ in the plane xy by an angle α about axis z of the reference frame (Fig. 2.5). Let (p'_x, p'_y, p'_z) be the coordinates of the vector $\boldsymbol{p}'$. The vector $\boldsymbol{p}$ has components

$$\begin{aligned} p_x &= p'_x \cos\alpha - p'_y \sin\alpha \\ p_y &= p'_x \sin\alpha + p'_y \cos\alpha \\ p_z &= p'_z. \end{aligned}$$

It is easy to recognize that $\boldsymbol{p}$ can be expressed as

$$\boldsymbol{p} = \boldsymbol{R}_z(\alpha)\boldsymbol{p}',$$

where $\boldsymbol{R}_z(\alpha)$ is the same rotation matrix as in (2.6).

In sum, a rotation matrix attains three *equivalent geometrical meanings*:

- It describes the mutual orientation between two coordinate frames; its column vectors are the direction cosines of the axes of the rotated frame with respect to the original frame.
- It represents the coordinate transformation between the coordinates of a point expressed in two different frames (with common origin).
- It is the operator that allows the rotation of a vector in the same coordinate frame.

2.3 Composition of Rotation Matrices

In order to derive composition rules of rotation matrices, it is useful to consider the expression of a vector in two different reference frames. Let then O–$x_0y_0z_0$,

O–$x_1y_1z_1$, O–$x_2y_2z_2$ be three frames with common origin O. The vector $\boldsymbol{p}$ describing the position of a generic point in space can be expressed in each of the above frames; let $\boldsymbol{p}^0$, $\boldsymbol{p}^1$, $\boldsymbol{p}^2$ denote the expressions of $\boldsymbol{p}$ in the three frames.[1]

At first, consider the relationship between the expression $\boldsymbol{p}^2$ of the vector $\boldsymbol{p}$ in Frame 2 and the expression $\boldsymbol{p}^1$ of the same vector in Frame 1. If $\boldsymbol{R}_i^j$ denotes the rotation matrix of Frame i with respect to Frame j, it is

$$\boldsymbol{p}^1 = \boldsymbol{R}_2^1 \boldsymbol{p}^2. \tag{2.12}$$

Similarly, it turns out that

$$\boldsymbol{p}^0 = \boldsymbol{R}_1^0 \boldsymbol{p}^1 \tag{2.13}$$

$$\boldsymbol{p}^0 = \boldsymbol{R}_2^0 \boldsymbol{p}^2. \tag{2.14}$$

On the other hand, substituting (2.12) in (2.13) and using (2.14) gives

$$\boldsymbol{R}_2^0 = \boldsymbol{R}_1^0 \boldsymbol{R}_2^1. \tag{2.15}$$

The relationship in (2.15) can be interpreted as the composition of successive rotations. Consider a frame initially aligned with the frame O–$x_0y_0z_0$. The rotation expressed by matrix $\boldsymbol{R}_2^0$ can be regarded as obtained in two steps:

- First rotate the given frame according to $\boldsymbol{R}_1^0$, so as to align it with frame O–$x_1y_1z_1$.
- Then rotate the frame, now aligned with frame O–$x_1y_1z_1$, according to $\boldsymbol{R}_2^1$, so as to align it with frame O–$x_2y_2z_2$.

Notice that the overall rotation can be expressed as a sequence of partial rotations; each rotation is defined with respect to the preceding one. The frame with respect to which the rotation occurs is termed *current frame*. Composition of successive rotations is then obtained by postmultiplication of the rotation matrices following the given order of rotations, as in (2.15). With the adopted notation, in view of (2.5), it is

$$\boldsymbol{R}_i^j = (\boldsymbol{R}_j^i)^{-1} = (\boldsymbol{R}_j^i)^T. \tag{2.16}$$

Successive rotations can be also specified by constantly referring them to the initial frame; in this case, the rotations are made with respect to a *fixed frame*. Let $\boldsymbol{R}_1^0$ be the rotation matrix of frame O–$x_1y_1z_1$ with respect to the fixed frame O–$x_0y_0z_0$. Let then $\bar{\boldsymbol{R}}_2^0$ denote the matrix characterizing frame O–$x_2y_2z_2$ with respect to Frame 0, which is obtained as a rotation of Frame 1 according to the matrix $\bar{\boldsymbol{R}}_2^1$. Since (2.15) gives a composition rule of successive rotations about the axes of the current frame, the overall rotation can be regarded as obtained in the following steps:

[1] Hereafter, the superscript of a vector or a matrix denotes the frame in which its components are expressed.

- First realign Frame 1 with Frame 0 by means of rotation $\boldsymbol{R}_0^1$.
- Then make the rotation expressed by $\bar{\boldsymbol{R}}_2^1$ with respect to the current frame.
- Finally compensate for the rotation made for the realignment by means of the inverse rotation $\boldsymbol{R}_1^0$.

Since the above rotations are described with respect to the current frame, the application of the composition rule (2.15) yields

$$\bar{\boldsymbol{R}}_2^0 = \boldsymbol{R}_1^0 \boldsymbol{R}_0^1 \bar{\boldsymbol{R}}_2^1 \boldsymbol{R}_1^0.$$

In view of (2.16), it is

$$\bar{\boldsymbol{R}}_2^0 = \bar{\boldsymbol{R}}_2^1 \boldsymbol{R}_1^0 \tag{2.17}$$

where the resulting $\bar{\boldsymbol{R}}_2^0$ is different from the matrix $\boldsymbol{R}_2^0$ in (2.15). Hence, it can be stated that composition of successive rotations with respect to a fixed frame is obtained by premultiplication of the single rotation matrices in the order of the given sequence of rotations.

By recalling the meaning of a rotation matrix in terms of the orientation of a current frame with respect to a fixed frame, it can be recognized that its columns are the direction cosines of the axes of the current frame with respect to the fixed frame, while its rows (columns of its transpose and inverse) are the direction cosines of the axes of the fixed frame with respect to the current frame.

An important issue of composition of rotations is that the matrix product is not commutative. In view of this, it can be concluded that two rotations in general do not commute and its composition depends on the order of the single rotations.

Example 2.3

Consider an object and a frame attached to it. Figure 2.6 shows the effects of two successive rotations of the object with respect to the current frame by changing the order of rotations. It is evident that the final object orientation is different in the two cases. Also in the case of rotations made with respect to the current frame, the final orientations differ (Fig. 2.7). It is interesting to note that the effects of the sequence of rotations with respect to the fixed frame are interchanged with the effects of the sequence of rotations with respect to the current frame. This can be explained by observing that the order of rotations in the fixed frame commutes with respect to the order of rotations in the current frame.

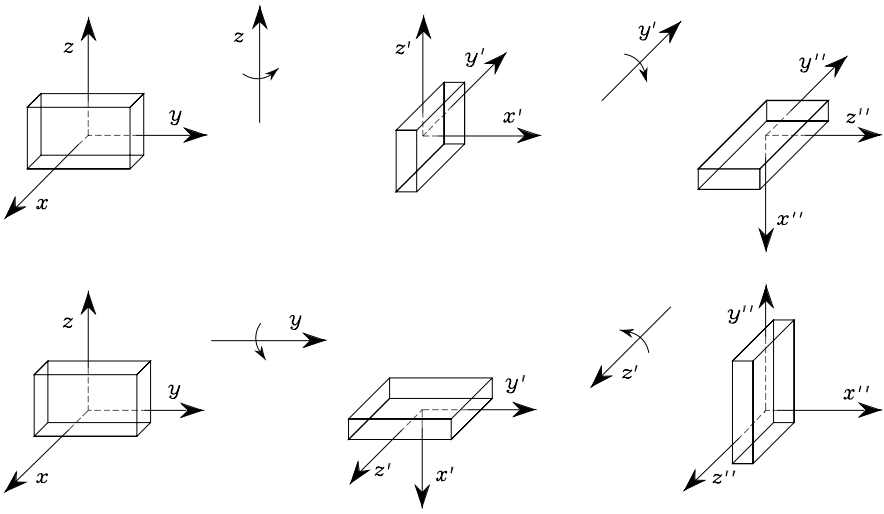

Fig. 2.6. Successive rotations of an object about axes of current frame

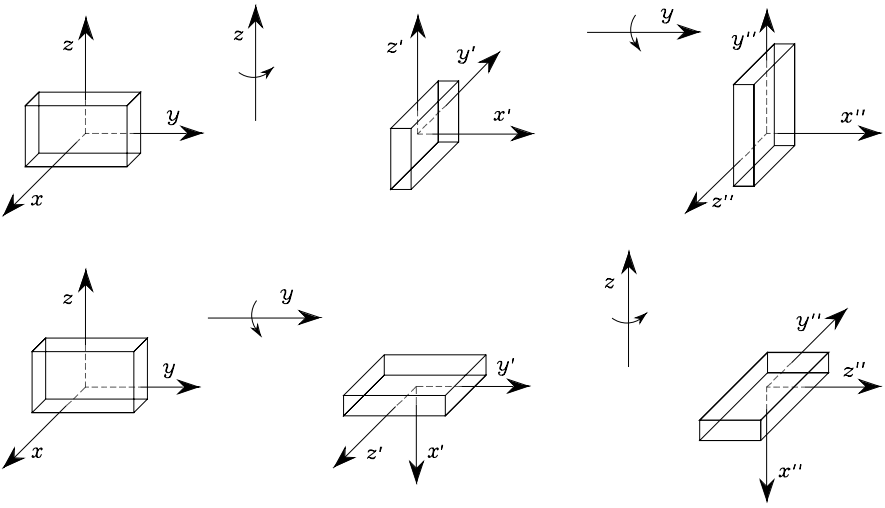

Fig. 2.7. Successive rotations of an object about axes of fixed frame

2.4 Euler Angles

Rotation matrices give a redundant description of frame orientation; in fact, they are characterized by nine elements which are not independent but related by six constraints due to the orthogonality conditions given in (2.4). This implies that *three parameters* are sufficient to describe orientation of a rigid body

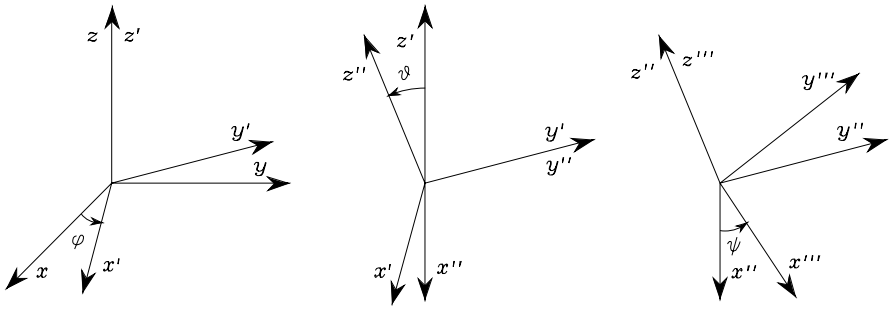

Fig. 2.8. Representation of Euler angles ZYZ

in space. A representation of orientation in terms of three independent parameters constitutes a *minimal representation*. In fact, a minimal representation of the special orthonormal group $SO(m)$ requires $m(m-1)/2$ parameters; thus, three parameters are needed to parameterize $SO(3)$, whereas only one parameter is needed for a planar rotation $SO(2)$.

A minimal representation of orientation can be obtained by using a set of three angles $\boldsymbol{\phi} = [\,\varphi \quad \vartheta \quad \psi\,]^T$. Consider the rotation matrix expressing the elementary rotation about one of the coordinate axes as a function of a single angle. Then, a generic rotation matrix can be obtained by composing a suitable sequence of three elementary rotations while guaranteeing that two successive rotations are not made about parallel axes. This implies that 12 distinct sets of angles are allowed out of all 27 possible combinations; each set represents a triplet of *Euler angles*. In the following, two sets of Euler angles are analyzed; namely, the ZYZ angles and the ZYX (or Roll–Pitch–Yaw) angles.

2.4.1 ZYZ Angles

The rotation described by *ZYZ angles* is obtained as composition of the following elementary rotations (Fig. 2.8):

- Rotate the reference frame by the angle φ about axis z; this rotation is described by the matrix $\boldsymbol{R}_z(\varphi)$ which is formally defined in (2.6).
- Rotate the current frame by the angle ϑ about axis y'; this rotation is described by the matrix $\boldsymbol{R}_{y'}(\vartheta)$ which is formally defined in (2.7).
- Rotate the current frame by the angle ψ about axis z''; this rotation is described by the matrix $\boldsymbol{R}_{z''}(\psi)$ which is again formally defined in (2.6).

The resulting frame orientation is obtained by composition of rotations with respect to *current frames*, and then it can be computed via postmultiplication of the matrices of elementary rotation, i.e.,[2]

$$\begin{aligned}\boldsymbol{R}(\boldsymbol{\phi}) &= \boldsymbol{R}_z(\varphi)\boldsymbol{R}_{y'}(\vartheta)\boldsymbol{R}_{z''}(\psi) \\ &= \begin{bmatrix} c_\varphi c_\vartheta c_\psi - s_\varphi s_\psi & -c_\varphi c_\vartheta s_\psi - s_\varphi c_\psi & c_\varphi s_\vartheta \\ s_\varphi c_\vartheta c_\psi + c_\varphi s_\psi & -s_\varphi c_\vartheta s_\psi + c_\varphi c_\psi & s_\varphi s_\vartheta \\ -s_\vartheta c_\psi & s_\vartheta s_\psi & c_\vartheta \end{bmatrix}.\end{aligned} \tag{2.18}$$

It is useful to solve the *inverse problem*, that is to determine the set of Euler angles corresponding to a given rotation matrix

$$\boldsymbol{R} = \begin{bmatrix} r_{11} & r_{12} & r_{13} \\ r_{21} & r_{22} & r_{23} \\ r_{31} & r_{32} & r_{33} \end{bmatrix}.$$

Compare this expression with that of $\boldsymbol{R}(\boldsymbol{\phi})$ in (2.18). By considering the elements $[1,3]$ and $[2,3]$, under the assumption that $r_{13} \neq 0$ and $r_{23} \neq 0$, it follows that

$$\varphi = \text{Atan2}(r_{23}, r_{13})$$

where $\text{Atan2}(y,x)$ is the arctangent function of two arguments[3]. Then, squaring and summing the elements $[1,3]$ and $[2,3]$ and using the element $[3,3]$ yields

$$\vartheta = \text{Atan2}\left(\sqrt{r_{13}^2 + r_{23}^2}, r_{33}\right).$$

The choice of the positive sign for the term $\sqrt{r_{13}^2 + r_{23}^2}$ limits the range of feasible values of ϑ to $(0,\pi)$. On this assumption, considering the elements $[3,1]$ and $[3,2]$ gives

$$\psi = \text{Atan2}(r_{32}, -r_{31}).$$

In sum, the requested solution is

$$\begin{aligned}\varphi &= \text{Atan2}(r_{23}, r_{13}) \\ \vartheta &= \text{Atan2}\left(\sqrt{r_{13}^2 + r_{23}^2}, r_{33}\right) \\ \psi &= \text{Atan2}(r_{32}, -r_{31}).\end{aligned} \tag{2.19}$$

It is possible to derive another solution which produces the same effects as solution (2.19). Choosing ϑ in the range $(-\pi, 0)$ leads to

$$\varphi = \text{Atan2}(-r_{23}, -r_{13})$$

[2] The notations c_ϕ and s_ϕ are the abbreviations for $\cos\phi$ and $\sin\phi$, respectively; short-hand notations of this kind will be adopted often throughout the text.

[3] The function $\text{Atan2}(y,x)$ computes the arctangent of the ratio y/x but utilizes the sign of each argument to determine which quadrant the resulting angle belongs to; this allows the correct determination of an angle in a range of 2π.

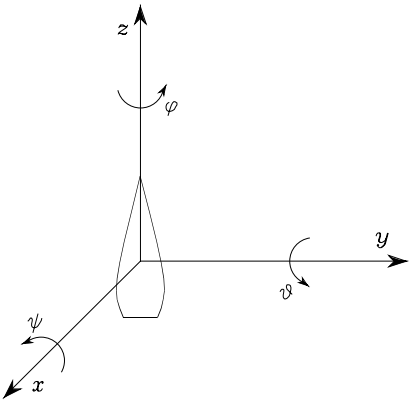

Fig. 2.9. Representation of Roll–Pitch–Yaw angles

$$\begin{aligned} \vartheta &= \mathrm{Atan2}\left(-\sqrt{r_{13}^2 + r_{23}^2}, r_{33}\right) \\ \psi &= \mathrm{Atan2}(-r_{32}, r_{31}). \end{aligned} \tag{2.20}$$

Solutions (2.19), (2.20) degenerate when $s_\vartheta = 0$; in this case, it is possible to determine only the sum or difference of φ and ψ. In fact, if $\vartheta = 0, \pi$, the successive rotations of φ and ψ are made about axes of current frames which are parallel, thus giving equivalent contributions to the rotation; see Problem 2.2.[4]

2.4.2 RPY Angles

Another set of Euler angles originates from a representation of orientation in the (aero)nautical field. These are the ZYX angles, also called *Roll–Pitch–Yaw angles*, to denote the typical changes of attitude of an (air)craft. In this case, the angles $\boldsymbol{\phi} = [\,\varphi \quad \vartheta \quad \psi\,]^T$ represent rotations defined with respect to a fixed frame attached to the centre of mass of the craft (Fig. 2.9).

The rotation resulting from Roll–Pitch–Yaw angles can be obtained as follows:

- Rotate the reference frame by the angle ψ about axis x (yaw); this rotation is described by the matrix $\boldsymbol{R}_x(\psi)$ which is formally defined in (2.8).
- Rotate the reference frame by the angle ϑ about axis y (pitch); this rotation is described by the matrix $\boldsymbol{R}_y(\vartheta)$ which is formally defined in (2.7).
- Rotate the reference frame by the angle φ about axis z (roll); this rotation is described by the matrix $\boldsymbol{R}_z(\varphi)$ which is formally defined in (2.6).

[4] In the following chapter, it will be seen that these configurations characterize the so-called representation *singularities* of the Euler angles.

The resulting frame orientation is obtained by composition of rotations with respect to the *fixed frame*, and then it can be computed via premultiplication of the matrices of elementary rotation, i.e.,[5]

$$\begin{aligned}\boldsymbol{R}(\boldsymbol{\phi}) &= \boldsymbol{R}_z(\varphi)\boldsymbol{R}_y(\vartheta)\boldsymbol{R}_x(\psi) \\ &= \begin{bmatrix} c_\varphi c_\vartheta & c_\varphi s_\vartheta s_\psi - s_\varphi c_\psi & c_\varphi s_\vartheta c_\psi + s_\varphi s_\psi \\ s_\varphi c_\vartheta & s_\varphi s_\vartheta s_\psi + c_\varphi c_\psi & s_\varphi s_\vartheta c_\psi - c_\varphi s_\psi \\ -s_\vartheta & c_\vartheta s_\psi & c_\vartheta c_\psi \end{bmatrix}.\end{aligned} \tag{2.21}$$

As for the Euler angles ZYZ, the *inverse solution* to a given rotation matrix

$$\boldsymbol{R} = \begin{bmatrix} r_{11} & r_{12} & r_{13} \\ r_{21} & r_{22} & r_{23} \\ r_{31} & r_{32} & r_{33} \end{bmatrix},$$

can be obtained by comparing it with the expression of $\boldsymbol{R}(\boldsymbol{\phi})$ in (2.21). The solution for ϑ in the range $(-\pi/2, \pi/2)$ is

$$\begin{aligned}\varphi &= \text{Atan2}(r_{21}, r_{11}) \\ \vartheta &= \text{Atan2}\left(-r_{31}, \sqrt{r_{32}^2 + r_{33}^2}\right) \\ \psi &= \text{Atan2}(r_{32}, r_{33}).\end{aligned} \tag{2.22}$$

The other equivalent solution for ϑ in the range $(\pi/2, 3\pi/2)$ is

$$\begin{aligned}\varphi &= \text{Atan2}(-r_{21}, -r_{11}) \\ \vartheta &= \text{Atan2}\left(-r_{31}, -\sqrt{r_{32}^2 + r_{33}^2}\right) \\ \psi &= \text{Atan2}(-r_{32}, -r_{33}).\end{aligned} \tag{2.23}$$

Solutions (2.22), (2.23) degenerate when $c_\vartheta = 0$; in this case, it is possible to determine only the sum or difference of φ and ψ.

2.5 Angle and Axis

A nonminimal representation of orientation can be obtained by resorting to *four parameters* expressing a rotation of a given angle about an axis in space. This can be advantageous in the problem of trajectory planning for a manipulator's end-effector orientation.

Let $\boldsymbol{r} = [\, r_x \quad r_y \quad r_z \,]^T$ be the unit vector of a rotation axis with respect to the reference frame O–xyz. In order to derive the rotation matrix $\boldsymbol{R}(\vartheta, \boldsymbol{r})$ expressing the rotation of an *angle* ϑ about *axis* $\boldsymbol{r}$, it is convenient to compose

[5] The ordered sequence of rotations XYZ about axes of the fixed frame is equivalent to the sequence ZYX about axes of the current frame.

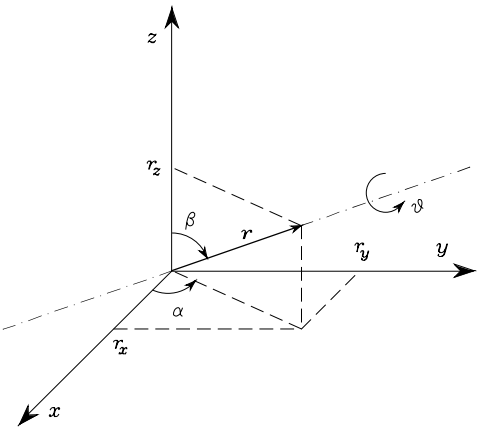

Fig. 2.10. Rotation of an angle about an axis

elementary rotations about the coordinate axes of the reference frame. The angle is taken to be positive if the rotation is made counter-clockwise about axis $\boldsymbol{r}$.

As shown in Fig. 2.10, a possible solution is to rotate first $\boldsymbol{r}$ by the angles necessary to align it with axis z, then to rotate by ϑ about z and finally to rotate by the angles necessary to align the unit vector with the initial direction. In detail, the sequence of rotations, to be made always with respect to axes of fixed frame, is the following:

- Align $\boldsymbol{r}$ with z, which is obtained as the sequence of a rotation by $-\alpha$ about z and a rotation by $-\beta$ about y.
- Rotate by ϑ about z.
- Realign with the initial direction of $\boldsymbol{r}$, which is obtained as the sequence of a rotation by β about y and a rotation by α about z.

In sum, the resulting rotation matrix is

$$\boldsymbol{R}(\vartheta, \boldsymbol{r}) = \boldsymbol{R}_z(\alpha)\boldsymbol{R}_y(\beta)\boldsymbol{R}_z(\vartheta)\boldsymbol{R}_y(-\beta)\boldsymbol{R}_z(-\alpha). \tag{2.24}$$

From the components of the unit vector $\boldsymbol{r}$ it is possible to extract the transcendental functions needed to compute the rotation matrix in (2.24), so as to eliminate the dependence from α and β; in fact, it is

$$\sin\alpha = \frac{r_y}{\sqrt{r_x^2 + r_y^2}} \qquad \cos\alpha = \frac{r_x}{\sqrt{r_x^2 + r_y^2}}$$

$$\sin\beta = \sqrt{r_x^2 + r_y^2} \qquad \cos\beta = r_z.$$

Then, it can be found that the rotation matrix corresponding to a given angle and axis is — see Problem 2.4 —

$$\boldsymbol{R}(\vartheta,\boldsymbol{r})=\begin{bmatrix} r_x^2(1-c_\vartheta)+c_\vartheta & r_xr_y(1-c_\vartheta)-r_zs_\vartheta & r_xr_z(1-c_\vartheta)+r_ys_\vartheta \\ r_xr_y(1-c_\vartheta)+r_zs_\vartheta & r_y^2(1-c_\vartheta)+c_\vartheta & r_yr_z(1-c_\vartheta)-r_xs_\vartheta \\ r_xr_z(1-c_\vartheta)-r_ys_\vartheta & r_yr_z(1-c_\vartheta)+r_xs_\vartheta & r_z^2(1-c_\vartheta)+c_\vartheta \end{bmatrix}. \tag{2.25}$$

For this matrix, the following property holds:

$$\boldsymbol{R}(-\vartheta,-\boldsymbol{r})=\boldsymbol{R}(\vartheta,\boldsymbol{r}), \tag{2.26}$$

i.e., a rotation by $-\vartheta$ about $-\boldsymbol{r}$ cannot be distinguished from a rotation by ϑ about $\boldsymbol{r}$; hence, such representation is not unique.

If it is desired to solve the *inverse problem* to compute the axis and angle corresponding to a given rotation matrix

$$\boldsymbol{R}=\begin{bmatrix} r_{11} & r_{12} & r_{13} \\ r_{21} & r_{22} & r_{23} \\ r_{31} & r_{32} & r_{33} \end{bmatrix},$$

the following result is useful:

$$\vartheta=\cos^{-1}\left(\frac{r_{11}+r_{22}+r_{33}-1}{2}\right) \tag{2.27}$$

$$\boldsymbol{r}=\frac{1}{2\sin\vartheta}\begin{bmatrix} r_{32}-r_{23} \\ r_{13}-r_{31} \\ r_{21}-r_{12} \end{bmatrix}, \tag{2.28}$$

for $\sin\vartheta\neq 0$. Notice that the expressions (2.27), (2.28) describe the rotation in terms of four parameters; namely, the angle and the three components of the axis unit vector. However, it can be observed that the three components of $\boldsymbol{r}$ are not independent but are constrained by the condition

$$r_x^2+r_y^2+r_z^2=1. \tag{2.29}$$

If $\sin\vartheta=0$, the expressions (2.27), (2.28) become meaningless. To solve the inverse problem, it is necessary to directly refer to the particular expressions attained by the rotation matrix $\boldsymbol{R}$ and find the solving formulae in the two cases $\vartheta=0$ and $\vartheta=\pi$. Notice that, when $\vartheta=0$ (null rotation), the unit vector $\boldsymbol{r}$ is arbitrary (singularity). See also Problem 2.5.

2.6 Unit Quaternion

The drawbacks of the angle/axis representation can be overcome by a different four-parameter representation; namely, the unit *quaternion*, viz. Euler parameters, defined as $\mathcal{Q}=\{\eta,\boldsymbol{\epsilon}\}$ where:

$$\eta=\cos\frac{\vartheta}{2} \tag{2.30}$$

$$\boldsymbol{\epsilon} = \sin\frac{\vartheta}{2}\,\boldsymbol{r}; \tag{2.31}$$

η is called the scalar part of the quaternion while $\boldsymbol{\epsilon} = [\,\epsilon_x \quad \epsilon_y \quad \epsilon_z\,]^T$ is called the vector part of the quaternion. They are constrained by the condition

$$\eta^2 + \epsilon_x^2 + \epsilon_y^2 + \epsilon_z^2 = 1, \tag{2.32}$$

hence, the name *unit* quaternion. It is worth remarking that, unlike the angle/axis representation, a rotation by $-\vartheta$ about $-\boldsymbol{r}$ gives the same quaternion as that associated with a rotation by ϑ about $\boldsymbol{r}$; this solves the above nonuniqueness problem. In view of (2.25), (2.30), (2.31), (2.32), the rotation matrix corresponding to a given quaternion takes on the form — see Problem 2.6 —

$$\boldsymbol{R}(\eta,\boldsymbol{\epsilon}) = \begin{bmatrix} 2(\eta^2+\epsilon_x^2)-1 & 2(\epsilon_x\epsilon_y-\eta\epsilon_z) & 2(\epsilon_x\epsilon_z+\eta\epsilon_y) \\ 2(\epsilon_x\epsilon_y+\eta\epsilon_z) & 2(\eta^2+\epsilon_y^2)-1 & 2(\epsilon_y\epsilon_z-\eta\epsilon_x) \\ 2(\epsilon_x\epsilon_z-\eta\epsilon_y) & 2(\epsilon_y\epsilon_z+\eta\epsilon_x) & 2(\eta^2+\epsilon_z^2)-1 \end{bmatrix}. \tag{2.33}$$

If it is desired to solve the *inverse problem* to compute the quaternion corresponding to a given rotation matrix

$$\boldsymbol{R} = \begin{bmatrix} r_{11} & r_{12} & r_{13} \\ r_{21} & r_{22} & r_{23} \\ r_{31} & r_{32} & r_{33} \end{bmatrix},$$

the following result is useful:

$$\eta = \frac{1}{2}\sqrt{r_{11}+r_{22}+r_{33}+1} \tag{2.34}$$

$$\boldsymbol{\epsilon} = \frac{1}{2}\begin{bmatrix} \mathrm{sgn}\,(r_{32}-r_{23})\sqrt{r_{11}-r_{22}-r_{33}+1} \\ \mathrm{sgn}\,(r_{13}-r_{31})\sqrt{r_{22}-r_{33}-r_{11}+1} \\ \mathrm{sgn}\,(r_{21}-r_{12})\sqrt{r_{33}-r_{11}-r_{22}+1} \end{bmatrix}, \tag{2.35}$$

where conventionally $\mathrm{sgn}\,(x) = 1$ for $x \geq 0$ and $\mathrm{sgn}\,(x) = -1$ for $x < 0$. Notice that in (2.34) it has been implicitly assumed $\eta \geq 0$; this corresponds to an angle $\vartheta \in [-\pi, \pi]$, and thus any rotation can be described. Also, compared to the inverse solution in (2.27), (2.28) for the angle and axis representation, no singularity occurs for (2.34), (2.35). See also Problem 2.8.

The quaternion extracted from $\boldsymbol{R}^{-1} = \boldsymbol{R}^T$ is denoted as $\mathcal{Q}^{-1}$, and can be computed as

$$\mathcal{Q}^{-1} = \{\eta, -\boldsymbol{\epsilon}\}. \tag{2.36}$$

Let $\mathcal{Q}_1 = \{\eta_1, \boldsymbol{\epsilon}_1\}$ and $\mathcal{Q}_2 = \{\eta_2, \boldsymbol{\epsilon}_2\}$ denote the quaternions corresponding to the rotation matrices $\boldsymbol{R}_1$ and $\boldsymbol{R}_2$, respectively. The quaternion corresponding to the product $\boldsymbol{R}_1\boldsymbol{R}_2$ is given by

$$\mathcal{Q}_1 * \mathcal{Q}_2 = \{\eta_1\eta_2 - \boldsymbol{\epsilon}_1^T\boldsymbol{\epsilon}_2, \eta_1\boldsymbol{\epsilon}_2 + \eta_2\boldsymbol{\epsilon}_1 + \boldsymbol{\epsilon}_1 \times \boldsymbol{\epsilon}_2\} \tag{2.37}$$

where the quaternion product operator "$*$" has been formally introduced. It is easy to see that if $\mathcal{Q}_2 = \mathcal{Q}_1^{-1}$ then the quaternion $\{1, \boldsymbol{0}\}$ is obtained from (2.37) which is the identity element for the product. See also Problem 2.9.

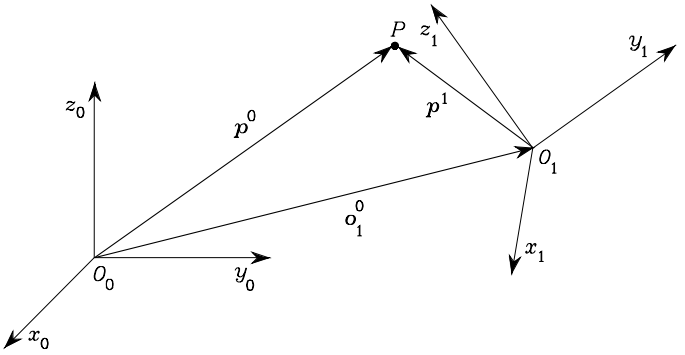

Fig. 2.11. Representation of a point P in different coordinate frames

2.7 Homogeneous Transformations

As illustrated at the beginning of the chapter, the position of a rigid body in space is expressed in terms of the position of a suitable point on the body with respect to a reference frame (translation), while its orientation is expressed in terms of the components of the unit vectors of a frame attached to the body — with origin in the above point — with respect to the same reference frame (rotation).

As shown in Fig. 2.11, consider an arbitrary point P in space. Let $\boldsymbol{p}^0$ be the vector of coordinates of P with respect to the reference frame O_0–$x_0y_0z_0$. Consider then another frame in space O_1–$x_1y_1z_1$. Let $\boldsymbol{o}_1^0$ be the vector describing the origin of Frame 1 with respect to Frame 0, and $\boldsymbol{R}_1^0$ be the rotation matrix of Frame 1 with respect to Frame 0. Let also $\boldsymbol{p}^1$ be the vector of coordinates of P with respect to Frame 1. On the basis of simple geometry, the position of point P with respect to the reference frame can be expressed as

$$\boldsymbol{p}^0 = \boldsymbol{o}_1^0 + \boldsymbol{R}_1^0 \boldsymbol{p}^1. \tag{2.38}$$

Hence, (2.38) represents the *coordinate transformation* (*translation* + *rotation*) of a bound vector between two frames.

The inverse transformation can be obtained by premultiplying both sides of (2.38) by $\boldsymbol{R}_1^{0T}$; in view of(2.4), it follows that

$$\boldsymbol{p}^1 = -\boldsymbol{R}_1^{0T} \boldsymbol{o}_1^0 + \boldsymbol{R}_1^{0T} \boldsymbol{p}^0 \tag{2.39}$$

which, via (2.16), can be written as

$$\boldsymbol{p}^1 = -\boldsymbol{R}_0^1 \boldsymbol{o}_1^0 + \boldsymbol{R}_0^1 \boldsymbol{p}^0. \tag{2.40}$$

In order to achieve a compact representation of the relationship between the coordinates of the same point in two different frames, the *homogeneous representation* of a generic vector $\boldsymbol{p}$ can be introduced as the vector $\tilde{\boldsymbol{p}}$ formed by adding a fourth unit component, i.e.,

$$\widetilde{\boldsymbol{p}} = \begin{bmatrix} \boldsymbol{p} \\ 1 \end{bmatrix}. \tag{2.41}$$

By adopting this representation for the vectors $\boldsymbol{p}^0$ and $\boldsymbol{p}^1$ in (2.38), the coordinate transformation can be written in terms of the (4×4) matrix

$$\boldsymbol{A}_1^0 = \begin{bmatrix} \boldsymbol{R}_1^0 & \boldsymbol{o}_1^0 \\ \boldsymbol{0}^T & 1 \end{bmatrix} \tag{2.42}$$

which, according to (2.41), is termed *homogeneous transformation matrix*. Since $\boldsymbol{o}_1^0 \in \mathbb{R}^3$ e $\boldsymbol{R}_1^0 \in SO(3)$, this matrix belongs to the *special Euclidean group* $SE(3) = \mathbb{R}^3 \times SO(3)$.

As can be easily seen from (2.42), the transformation of a vector from Frame 1 to Frame 0 is expressed by a single matrix containing the rotation matrix of Frame 1 with respect to Frame 0 and the translation vector from the origin of Frame 0 to the origin of Frame 1.[6] Therefore, the coordinate transformation (2.38) can be compactly rewritten as

$$\widetilde{\boldsymbol{p}}^0 = \boldsymbol{A}_1^0 \widetilde{\boldsymbol{p}}^1. \tag{2.43}$$

The coordinate transformation between Frame 0 and Frame 1 is described by the homogeneous transformation matrix $\boldsymbol{A}_0^1$ which satisfies the equation

$$\widetilde{\boldsymbol{p}}^1 = \boldsymbol{A}_0^1 \widetilde{\boldsymbol{p}}^0 = \left(\boldsymbol{A}_1^0\right)^{-1} \widetilde{\boldsymbol{p}}^0. \tag{2.44}$$

This matrix is expressed in a block-partitioned form as

$$\boldsymbol{A}_0^1 = \begin{bmatrix} \boldsymbol{R}_1^{0T} & -\boldsymbol{R}_1^{0T}\boldsymbol{o}_1^0 \\ \boldsymbol{0}^T & 1 \end{bmatrix} = \begin{bmatrix} \boldsymbol{R}_0^1 & -\boldsymbol{R}_0^1\boldsymbol{o}_1^0 \\ \boldsymbol{0}^T & 1 \end{bmatrix}, \tag{2.45}$$

which gives the homogeneous representation form of the result already established by (2.39), (2.40) — see Problem 2.10.

Notice that for the homogeneous transformation matrix the orthogonality property does not hold; hence, in general,

$$\boldsymbol{A}^{-1} \neq \boldsymbol{A}^T. \tag{2.46}$$

In sum, a homogeneous transformation matrix expresses the coordinate transformation between two frames in a compact form. If the frames have the

[6] It can be shown that in (2.42) non-null values of the first three elements of the fourth row of $\boldsymbol{A}$ produce a perspective effect, while values other than unity for the fourth element give a scaling effect.

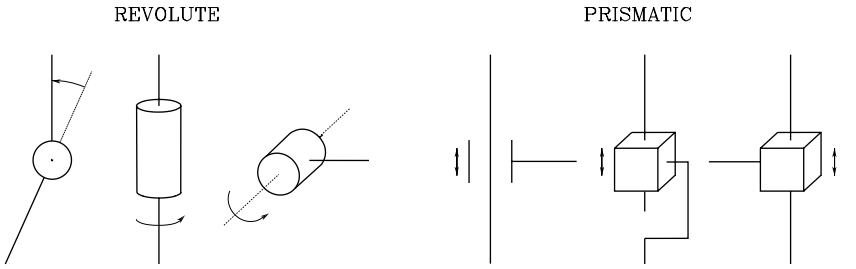

Fig. 2.12. Conventional representations of joints

same origin, it reduces to the rotation matrix previously defined. Instead, if the frames have distinct origins, it allows the notation with superscripts and subscripts to be kept which directly characterize the current frame and the fixed frame.

Analogously to what presented for the rotation matrices, it is easy to verify that a sequence of coordinate transformations can be composed by the product

$$\widetilde{\boldsymbol{p}}^0 = \boldsymbol{A}_1^0 \boldsymbol{A}_2^1 \dots \boldsymbol{A}_n^{n-1} \widetilde{\boldsymbol{p}}^n \tag{2.47}$$

where $\boldsymbol{A}_i^{i-1}$ denotes the homogeneous transformation relating the description of a point in Frame i to the description of the same point in Frame $i-1$.

2.8 Direct Kinematics

A manipulator consists of a series of rigid bodies (*links*) connected by means of kinematic pairs or *joints*. Joints can be essentially of two types: *revolute* and *prismatic*; conventional representations of the two types of joints are sketched in Fig. 2.12. The whole structure forms a *kinematic chain*. One end of the chain is constrained to a base. An *end-effector* (gripper, tool) is connected to the other end allowing manipulation of objects in space.

From a topological viewpoint, the kinematic chain is termed *open* when there is only one sequence of links connecting the two ends of the chain. Alternatively, a manipulator contains a *closed* kinematic chain when a sequence of links forms a loop.

The mechanical structure of a manipulator is characterized by a number of degrees of freedom (DOFs) which uniquely determine its *posture*.[7] Each DOF is typically associated with a joint articulation and constitutes a *joint variable*. The aim of *direct kinematics* is to compute the pose of the end-effector as a function of the joint variables.

[7] The term *posture* of a kinematic chain denotes the pose of all the rigid bodies composing the chain. Whenever the kinematic chain reduces to a single rigid body, then the posture coincides with the pose of the body.

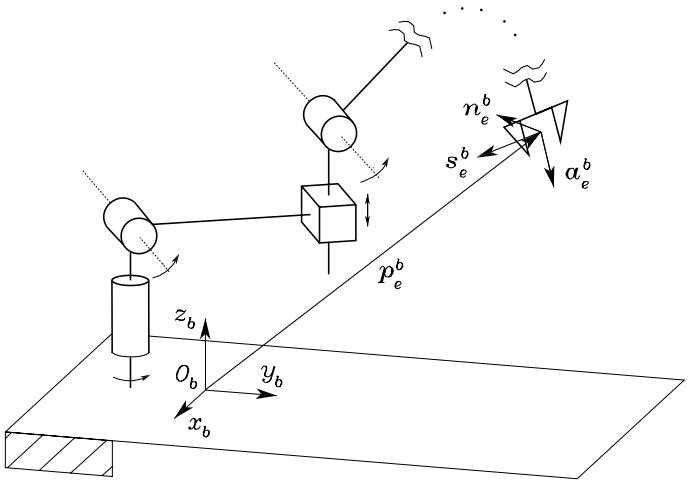

Fig. 2.13. Description of the position and orientation of the end-effector frame

It was previously illustrated that the pose of a body with respect to a reference frame is described by the position vector of the origin and the unit vectors of a frame attached to the body. Hence, with respect to a reference frame O_b–$x_by_bz_b$, the direct kinematics function is expressed by the homogeneous transformation matrix

$$\boldsymbol{T}_e^b(\boldsymbol{q}) = \begin{bmatrix} \boldsymbol{n}_e^b(\boldsymbol{q}) & \boldsymbol{s}_e^b(\boldsymbol{q}) & \boldsymbol{a}_e^b(\boldsymbol{q}) & \boldsymbol{p}_e^b(\boldsymbol{q}) \\ 0 & 0 & 0 & 1 \end{bmatrix}, \tag{2.48}$$

where $\boldsymbol{q}$ is the $(n \times 1)$ vector of joint variables, $\boldsymbol{n}_e$, $\boldsymbol{s}_e$, $\boldsymbol{a}_e$ are the unit vectors of a frame attached to the end-effector, and $\boldsymbol{p}_e$ is the position vector of the origin of such a frame with respect to the origin of the base frame O_b–$x_by_bz_b$ (Fig. 2.13). Note that $\boldsymbol{n}_e$, $\boldsymbol{s}_e$, $\boldsymbol{a}_e$ and $\boldsymbol{p}_e$ are a function of $\boldsymbol{q}$.

The frame O_b–$x_by_bz_b$ is termed *base frame*. The frame attached to the end-effector is termed *end-effector frame* and is conveniently chosen according to the particular task geometry. If the end-effector is a gripper, the origin of the end-effector frame is located at the centre of the gripper, the unit vector $\boldsymbol{a}_e$ is chosen in the *approach* direction to the object, the unit vector $\boldsymbol{s}_e$ is chosen normal to $\boldsymbol{a}_e$ in the *sliding* plane of the jaws, and the unit vector $\boldsymbol{n}_e$ is chosen *normal* to the other two so that the frame $(\boldsymbol{n}_e, \boldsymbol{s}_e, \boldsymbol{a}_e)$ is right-handed.

A first way to compute direct kinematics is offered by a geometric analysis of the structure of the given manipulator.

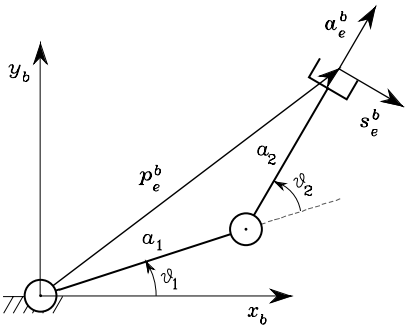

Fig. 2.14. Two-link planar arm

Example 2.4

Consider the two-link planar arm in Fig. 2.14. On the basis of simple trigonometry, the choice of the joint variables, the base frame, and the end-effector frame leads to[8]

$$\boldsymbol{T}_e^b(\boldsymbol{q}) = \begin{bmatrix} \boldsymbol{n}_e^b & \boldsymbol{s}_e^b & \boldsymbol{a}_e^b & \boldsymbol{p}_e^b \\ 0 & 0 & 0 & 1 \end{bmatrix} = \begin{bmatrix} 0 & s_{12} & c_{12} & a_1 c_1 + a_2 c_{12} \\ 0 & -c_{12} & s_{12} & a_1 s_1 + a_2 s_{12} \\ 1 & 0 & 0 & 0 \\ 0 & 0 & 0 & 1 \end{bmatrix}. \tag{2.49}$$

It is not difficult to infer that the effectiveness of a geometric approach to the direct kinematics problem is based first on a convenient choice of the relevant quantities and then on the ability and geometric intuition of the problem solver. Whenever the manipulator structure is complex and the number of joints increases, it is preferable to adopt a less direct solution, which, though, is based on a systematic, general procedure. The problem becomes even more complex when the manipulator contains one or more closed kinematic chains. In such a case, as it will be discussed later, there is no guarantee to obtain an analytical expression for the direct kinematics function in (2.48).

2.8.1 Open Chain

Consider an *open-chain* manipulator constituted by $n+1$ links connected by n joints, where Link 0 is conventionally fixed to the ground. It is assumed that each joint provides the mechanical structure with a single DOF, corresponding to the joint variable.

The construction of an operating procedure for the computation of direct kinematics is naturally derived from the typical open kinematic chain of the manipulator structure. In fact, since each joint connects two consecutive

[8] The notations $s_{i\ldots j}$, $c_{i\ldots j}$ denote respectively $\sin(q_i + \ldots + q_j)$, $\cos(q_i + \ldots + q_j)$.

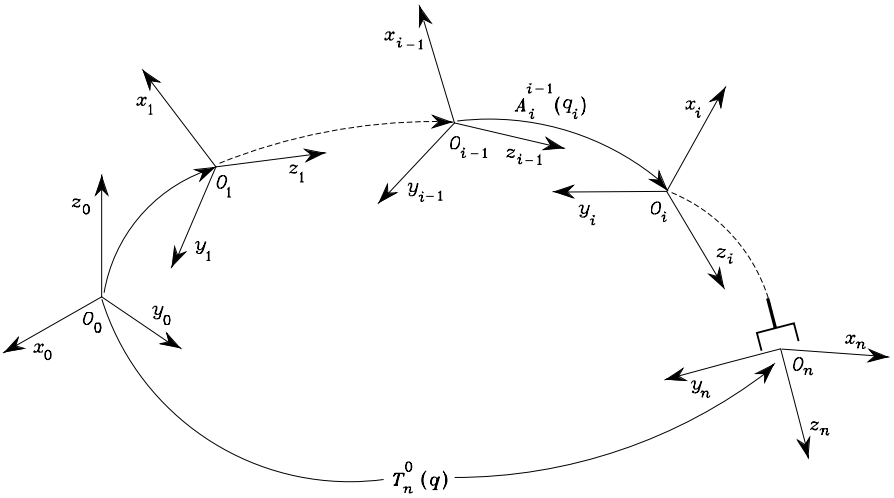

Fig. 2.15. Coordinate transformations in an open kinematic chain

links, it is reasonable to consider first the description of kinematic relationship between consecutive links and then to obtain the overall description of manipulator kinematics in a recursive fashion. To this purpose, it is worth defining a coordinate frame attached to each link, from Link 0 to Link n. Then, the coordinate transformation describing the position and orientation of Frame n with respect to Frame 0 (Fig. 2.15) is given by

$$\boldsymbol{T}_n^0(\boldsymbol{q}) = \boldsymbol{A}_1^0(q_1)\boldsymbol{A}_2^1(q_2)\dots\boldsymbol{A}_n^{n-1}(q_n). \tag{2.50}$$

As requested, the computation of the direct kinematics function is recursive and is obtained in a systematic manner by simple products of the homogeneous transformation matrices $\boldsymbol{A}_i^{i-1}(q_i)$ (for $i = 1, \dots, n$), each of which is a function of a single joint variable.

With reference to the direct kinematics equation in (2.49), the actual coordinate transformation describing the position and orientation of the end-effector frame with respect to the base frame can be obtained as

$$\boldsymbol{T}_e^b(\boldsymbol{q}) = \boldsymbol{T}_0^b\boldsymbol{T}_n^0(\boldsymbol{q})\boldsymbol{T}_e^n \tag{2.51}$$

where $\boldsymbol{T}_0^b$ and $\boldsymbol{T}_e^n$ are two (typically) constant homogeneous transformations describing the position and orientation of Frame 0 with respect to the base frame, and of the end-effector frame with respect to Frame n, respectively.

2.8.2 Denavit–Hartenberg Convention

In order to compute the direct kinematics equation for an open-chain manipulator according to the recursive expression in (2.50), a systematic, general

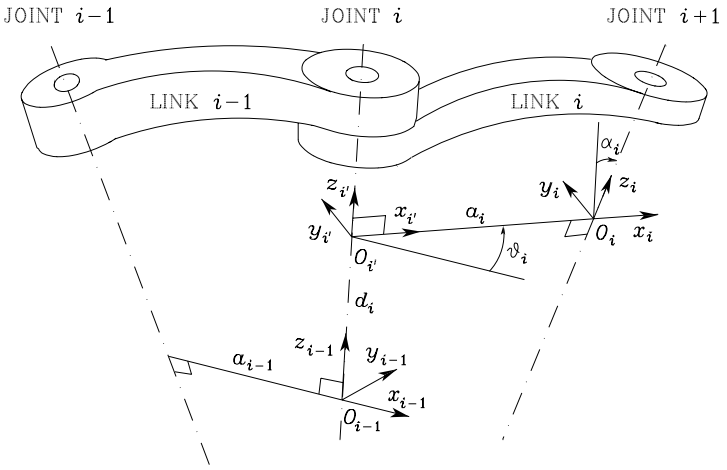

Fig. 2.16. Denavit–Hartenberg kinematic parameters

method is to be derived to define the relative position and orientation of two consecutive links; the problem is that of determining two frames attached to the two links and computing the coordinate transformations between them. In general, the frames can be arbitrarily chosen as long as they are attached to the link they are referred to. Nevertheless, it is convenient to set some rules also for the definition of the link frames.

With reference to Fig. 2.16, let Axis i denote the axis of the joint connecting Link $i-1$ to Link i; the so-called *Denavit–Hartenberg convention* (DH) is adopted to define link Frame i:

- Choose axis z_i along the axis of Joint $i+1$.
- Locate the origin O_i at the intersection of axis z_i with the common normal[9] to axes z_{i-1} and z_i. Also, locate $O_{i'}$ at the intersection of the common normal with axis z_{i-1}.
- Choose axis x_i along the common normal to axes z_{i-1} and z_i with positive direction from Joint i to Joint $i+1$.
- Choose axis y_i so as to complete a right-handed frame.

The Denavit–Hartenberg convention gives a nonunique definition of the link frame in the following cases:

- For Frame 0, only the direction of axis z_0 is specified; then O_0 and x_0 can be arbitrarily chosen.
- For Frame n, since there is no Joint $n+1$, z_n is not uniquely defined while x_n has to be normal to axis z_{n-1}. Typically, Joint n is revolute, and thus z_n can be aligned with the direction of z_{n-1}.

[9] The common normal between two lines is the line containing the minimum distance segment between the two lines.

- When two consecutive axes are parallel, the common normal between them is not uniquely defined.
- When two consecutive axes intersect, the positive direction of x_i is arbitrary.
- When Joint i is prismatic, only the direction of z_{i-1} is specified.

In all such cases, the indeterminacy can be exploited to simplify the procedure; for instance, the axes of consecutive frames can be made parallel.

Once the link frames have been established, the position and orientation of Frame i with respect to Frame $i-1$ are completely specified by the following *parameters*:

a_i distance between O_i and $O_{i'}$,
d_i coordinate of $O_{i'}$ along z_{i-1},
α_i angle between axes z_{i-1} and z_i about axis x_i to be taken positive when rotation is made counter-clockwise,
ϑ_i angle between axes x_{i-1} and x_i about axis z_{i-1} to be taken positive when rotation is made counter-clockwise.

Two of the four parameters (a_i and α_i) are always constant and depend only on the geometry of connection between consecutive joints established by Link i. Of the remaining two parameters, only one is variable depending on the type of joint that connects Link $i-1$ to Link i. In particular:

- if Joint i is *revolute* the variable is ϑ_i,
- if Joint i is *prismatic* the variable is d_i.

At this point, it is possible to express the coordinate transformation between Frame i and Frame $i-1$ according to the following steps:

- Choose a frame aligned with Frame $i-1$.
- Translate the chosen frame by d_i along axis z_{i-1} and rotate it by ϑ_i about axis z_{i-1}; this sequence aligns the current frame with Frame i' and is described by the homogeneous transformation matrix

$$\boldsymbol{A}_{i'}^{i-1} = \begin{bmatrix} c_{\vartheta_i} & -s_{\vartheta_i} & 0 & 0 \\ s_{\vartheta_i} & c_{\vartheta_i} & 0 & 0 \\ 0 & 0 & 1 & d_i \\ 0 & 0 & 0 & 1 \end{bmatrix}.$$

- Translate the frame aligned with Frame i' by a_i along axis $x_{i'}$ and rotate it by α_i about axis $x_{i'}$; this sequence aligns the current frame with Frame i and is described by the homogeneous transformation matrix

$$\boldsymbol{A}_{i}^{i'} = \begin{bmatrix} 1 & 0 & 0 & a_i \\ 0 & c_{\alpha_i} & -s_{\alpha_i} & 0 \\ 0 & s_{\alpha_i} & c_{\alpha_i} & 0 \\ 0 & 0 & 0 & 1 \end{bmatrix}.$$

- The resulting coordinate transformation is obtained by postmultiplication of the single transformations as

$$\boldsymbol{A}_i^{i-1}(q_i) = \boldsymbol{A}_{i'}^{i-1}\boldsymbol{A}_i^{i'} = \begin{bmatrix} c_{\vartheta_i} & -s_{\vartheta_i}c_{\alpha_i} & s_{\vartheta_i}s_{\alpha_i} & a_i c_{\vartheta_i} \\ s_{\vartheta_i} & c_{\vartheta_i}c_{\alpha_i} & -c_{\vartheta_i}s_{\alpha_i} & a_i s_{\vartheta_i} \\ 0 & s_{\alpha_i} & c_{\alpha_i} & d_i \\ 0 & 0 & 0 & 1 \end{bmatrix}. \tag{2.52}$$

Notice that the transformation matrix from Frame i to Frame $i-1$ is a function only of the joint variable q_i, that is, ϑ_i for a revolute joint or d_i for a prismatic joint.

To summarize, the Denavit–Hartenberg convention allows the construction of the direct kinematics function by composition of the individual coordinate transformations expressed by (2.52) into one homogeneous transformation matrix as in (2.50). The procedure can be applied to any open kinematic chain and can be easily rewritten in an operating form as follows.

1. Find and number consecutively the joint axes; set the directions of axes $z_0, \ldots, z_{n-1}$.
2. Choose Frame 0 by locating the origin on axis z_0; axes x_0 and y_0 are chosen so as to obtain a right-handed frame. If feasible, it is worth choosing Frame 0 to coincide with the base frame.

Execute steps from **3** to **5** for $i = 1, \ldots, n-1$:

3. Locate the origin O_i at the intersection of z_i with the common normal to axes z_{i-1} and z_i. If axes z_{i-1} and z_i are parallel and Joint i is revolute, then locate O_i so that $d_i = 0$; if Joint i is prismatic, locate O_i at a reference position for the joint range, e.g., a mechanical limit.
4. Choose axis x_i along the common normal to axes z_{i-1} and z_i with direction from Joint i to Joint $i+1$.
5. Choose axis y_i so as to obtain a right-handed frame.

To complete:

6. Choose Frame n; if Joint n is revolute, then align z_n with z_{n-1}, otherwise, if Joint n is prismatic, then choose z_n arbitrarily. Axis x_n is set according to step **4**.
7. For $i = 1, \ldots, n$, form the table of parameters $a_i, d_i, \alpha_i, \vartheta_i$.
8. On the basis of the parameters in **7**, compute the homogeneous transformation matrices $\boldsymbol{A}_i^{i-1}(q_i)$ for $i = 1, \ldots, n$.
9. Compute the homogeneous transformation $\boldsymbol{T}_n^0(\boldsymbol{q}) = \boldsymbol{A}_1^0 \ldots \boldsymbol{A}_n^{n-1}$ that yields the position and orientation of Frame n with respect to Frame 0.
10. Given $\boldsymbol{T}_0^b$ and $\boldsymbol{T}_e^n$, compute the direct kinematics function as $\boldsymbol{T}_e^b(\boldsymbol{q}) = \boldsymbol{T}_0^b\boldsymbol{T}_n^0\boldsymbol{T}_e^n$ that yields the position and orientation of the end-effector frame with respect to the base frame.

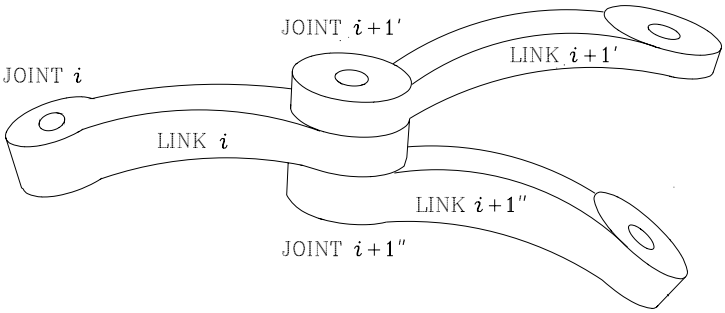

Fig. 2.17. Connection of a single link in the chain with two links

For what concerns the computational aspects of direct kinematics, it can be recognized that the heaviest load derives from the evaluation of transcendental functions. On the other hand, by suitably factorizing the transformation equations and introducing local variables, the number of flops (additions + multiplications) can be reduced. Finally, for computation of orientation it is convenient to evaluate the two unit vectors of the end-effector frame of simplest expression and derive the third one by vector product of the first two.

2.8.3 Closed Chain

The above direct kinematics method based on the DH convention exploits the inherently recursive feature of an open-chain manipulator. Nevertheless, the method can be extended to the case of manipulators containing closed kinematic chains according to the technique illustrated below.

Consider a *closed-chain* manipulator constituted by $n+1$ links. Because of the presence of a loop, the number of joints l must be greater than n; in particular, it can be understood that the number of closed loops is equal to $l-n$.

With reference to Fig. 2.17, Links 0 through i are connected successively through the first i joints as in an open kinematic chain. Then, Joint $i+1'$ connects Link i with Link $i+1'$ while Joint $i+1''$ connects Link i with Link $i+1''$; the axes of Joints $i+1'$ and $i+1''$ are assumed to be aligned. Although not represented in the figure, Links $i+1'$ and $i+1''$ are members of the closed kinematic chain. In particular, Link $i+1'$ is further connected to Link $i+2'$ via Joint $i+2'$ and so forth, until Link j via Joint j. Likewise, Link $i+1''$ is further connected to Link $i+2''$ via Joint $i+2''$ and so forth, until Link k via Joint k. Finally, Links j and k are connected together at Joint $j+1$ to form a closed chain. In general, $j \neq k$.

In order to attach frames to the various links and apply DH convention, one closed kinematic chain is taken into account. The closed chain can be virtually cut open at Joint $j+1$, i.e., the joint between Link j and Link k. An equivalent tree-structured open kinematic chain is obtained, and thus link

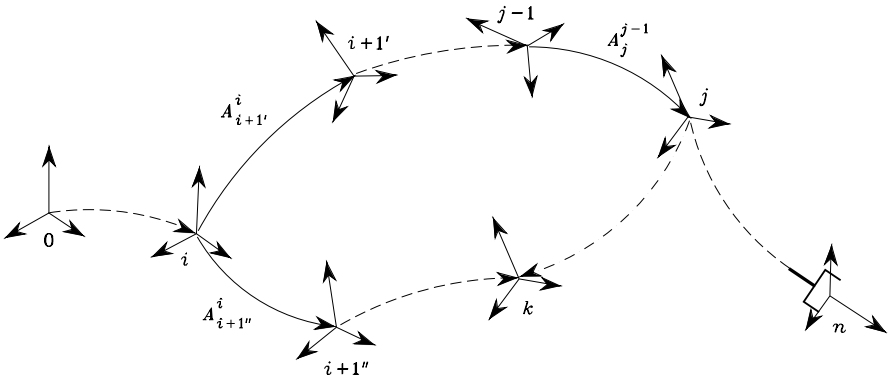

Fig. 2.18. Coordinate transformations in a closed kinematic chain

frames can be defined as in Fig. 2.18. Since Links 0 through i occur before the two branches of the tree, they are left out of the analysis. For the same reason, Links $j+1$ through n are left out as well. Notice that Frame i is to be chosen with axis z_i aligned with the axes of Joints $i+1'$ and $i+1''$.

It follows that the position and orientation of Frame j with respect to Frame i can be expressed by composing the homogeneous transformations as

$$\boldsymbol{A}_j^i(\boldsymbol{q}') = \boldsymbol{A}_{i+1'}^i(q_{i+1'}) \dots \boldsymbol{A}_j^{j-1}(q_j) \tag{2.53}$$

where $\boldsymbol{q}' = [\, q_{i+1'} \quad \dots \quad q_j \,]^T$. Likewise, the position and orientation of Frame k with respect to Frame i is given by

$$\boldsymbol{A}_k^i(\boldsymbol{q}'') = \boldsymbol{A}_{i+1''}^i(q_{i+1''}) \dots \boldsymbol{A}_k^{k-1}(q_k) \tag{2.54}$$

where $\boldsymbol{q}'' = [\, q_{i+1''} \quad \dots \quad q_k \,]^T$.

Since Links j and k are connected to each other through Joint $j+1$, it is worth analyzing the mutual position and orientation between Frames j and k, as illustrated in Fig. 2.19. Notice that, since Links j and k are connected to form a closed chain, axes z_j and z_k are aligned. Therefore, the following orientation constraint has to be imposed between Frames j and k:

$$\boldsymbol{z}_j^i(\boldsymbol{q}') = \boldsymbol{z}_k^i(\boldsymbol{q}''), \tag{2.55}$$

where the unit vectors of the two axes have been conveniently referred to Frame i.

Moreover, if Joint $j+1$ is prismatic, the angle ϑ_{jk} between axes x_j and x_k is fixed; hence, in addition to (2.55), the following constraint is obtained:

$$\boldsymbol{x}_j^{iT}(\boldsymbol{q}')\boldsymbol{x}_k^i(\boldsymbol{q}'') = \cos\vartheta_{jk}. \tag{2.56}$$

Obviously, there is no need to impose a similar constraint on axes y_j and y_k since that would be redundant.

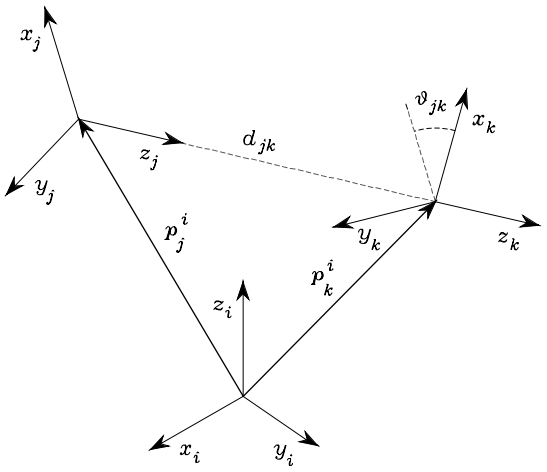

Fig. 2.19. Coordinate transformation at the cut joint

Regarding the position constraint between Frames j and k, let $\boldsymbol{p}_j^i$ and $\boldsymbol{p}_k^i$ respectively denote the positions of the origins of Frames j and k, when referred to Frame i. By projecting on Frame j the distance vector of the origin of Frame k from Frame j, the following constraint has to be imposed:

$$\boldsymbol{R}_i^j(\boldsymbol{q}')\left(\boldsymbol{p}_j^i(\boldsymbol{q}') - \boldsymbol{p}_k^i(\boldsymbol{q}'')\right) = [\,0 \quad 0 \quad d_{jk}\,]^T \tag{2.57}$$

where $\boldsymbol{R}_i^j = \boldsymbol{R}_j^{iT}$ denotes the orientation of Frame i with respect to Frame j. At this point, if Joint $j+1$ is revolute, then d_{jk} is a fixed offset along axis z_j; hence, the three equalities of (2.57) fully describe the position constraint. If, however, Joint $j+1$ is prismatic, then d_{jk} varies. Consequently, only the first two equalities of (2.57) describe the position constraint, i.e.,

$$\begin{bmatrix} \boldsymbol{x}_j^{iT}(\boldsymbol{q}') \\ \boldsymbol{y}_j^{iT}(\boldsymbol{q}') \end{bmatrix} \left(\boldsymbol{p}_j^i(\boldsymbol{q}') - \boldsymbol{p}_k^i(\boldsymbol{q}'')\right) = \begin{bmatrix} 0 \\ 0 \end{bmatrix} \tag{2.58}$$

where $\boldsymbol{R}_j^i = [\,\boldsymbol{x}_j^i \quad \boldsymbol{y}_j^i \quad \boldsymbol{z}_j^i\,]$.

In summary, if Joint $j+1$ is *revolute* the constraints are

$$\begin{cases} \boldsymbol{R}_i^j(\boldsymbol{q}')\left(\boldsymbol{p}_j^i(\boldsymbol{q}') - \boldsymbol{p}_k^i(\boldsymbol{q}'')\right) = [\,0 \quad 0 \quad d_{jk}\,]^T \\ \boldsymbol{z}_j^i(\boldsymbol{q}') = \boldsymbol{z}_k^i(\boldsymbol{q}''), \end{cases} \tag{2.59}$$

whereas if Joint $j+1$ is *prismatic* the constraints are

$$\begin{cases} \begin{bmatrix} \boldsymbol{x}_j^{iT}(\boldsymbol{q}') \\ \boldsymbol{y}_j^{iT}(\boldsymbol{q}') \end{bmatrix} \left(\boldsymbol{p}_j^i(\boldsymbol{q}') - \boldsymbol{p}_k^i(\boldsymbol{q}'')\right) = \begin{bmatrix} 0 \\ 0 \end{bmatrix} \\ \boldsymbol{z}_j^i(\boldsymbol{q}') = \boldsymbol{z}_k^i(\boldsymbol{q}'') \\ \boldsymbol{x}_j^{iT}(\boldsymbol{q}')\boldsymbol{x}_k^i(\boldsymbol{q}'') = \cos\vartheta_{jk}. \end{cases} \tag{2.60}$$

In either case, there are six equalities that must be satisfied. Those should be solved for a reduced number of independent joint variables to be keenly chosen among the components of $\boldsymbol{q}'$ and $\boldsymbol{q}''$ which characterize the DOFs of the closed chain. These are the natural candidates to be the actuated joints, while the other joints in the chain (including the cut joint) are typically not actuated. Such independent variables, together with the remaining joint variables not involved in the above analysis, constitute the joint vector $\boldsymbol{q}$ that allows the direct kinematics equation to be computed as

$$\boldsymbol{T}_n^0(\boldsymbol{q}) = \boldsymbol{A}_i^0 \boldsymbol{A}_j^i \boldsymbol{A}_n^j, \tag{2.61}$$

where the sequence of successive transformations after the closure of the chain has been conventionally resumed from Frame j.

In general, there is no guarantee to solve the constraints in closed form unless the manipulator has a simple kinematic structure. In other words, for a given manipulator with a specific geometry, e.g., a planar structure, some of the above equalities may become dependent. Hence, the number of independent equalities is less than six and it should likely be easier to solve them.

To conclude, it is worth sketching the operating form of the procedure to compute the direct kinematics function for a closed-chain manipulator using the Denavit–Hartenberg convention.

1. In the closed chain, select one joint that is not actuated. Assume that the joint is cut open so as to obtain an open chain in a tree structure.
2. Compute the homogeneous transformations according to DH convention.
3. Find the equality constraints for the two frames connected by the cut joint.
4. Solve the constraints for a reduced number of joint variables.
5. Express the homogeneous transformations in terms of the above joint variables and compute the direct kinematics function by composing the various transformations from the base frame to the end-effector frame.

2.9 Kinematics of Typical Manipulator Structures

This section contains several examples of computation of the direct kinematics function for typical manipulator structures that are often encountered in industrial robots.

With reference to the schematic representation of the kinematic chain, manipulators are usually illustrated in postures where the joint variables, defined according to the DH convention, are different from zero; such values might differ from the null references utilized for robot manipulator programming. Hence, it will be necessary to sum constant contributions (offsets) to the values of the joint variables measured by the robot sensory system, so as to match the references.

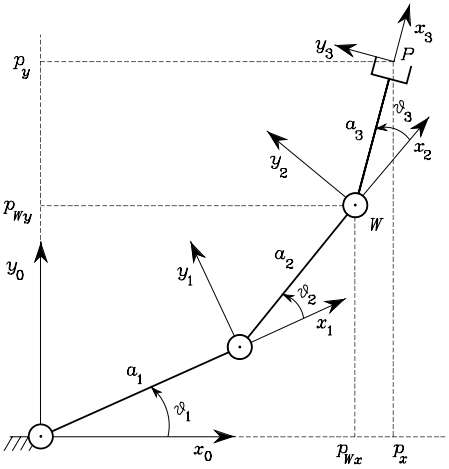

Fig. 2.20. Three-link planar arm

2.9.1 Three-link Planar Arm

Consider the three-link planar arm in Fig. 2.20, where the link frames have been illustrated. Since the revolute axes are all parallel, the simplest choice was made for all axes x_i along the direction of the relative links (the direction of x_0 is arbitrary) and all lying in the plane (x_0, y_0). In this way, all the parameters d_i are null and the angles between the axes x_i directly provide the joint variables. The DH parameters are specified in Table 2.1.

Table 2.1. DH parameters for the three-link planar arm

Link	a_i	α_i	d_i	ϑ_i
1	a_1	0	0	ϑ_1
2	a_2	0	0	ϑ_2
3	a_3	0	0	ϑ_3

Since all joints are revolute, the homogeneous transformation matrix defined in (2.52) has the same structure for each joint, i.e.,

$$\boldsymbol{A}_i^{i-1}(\vartheta_i) = \begin{bmatrix} c_i & -s_i & 0 & a_i c_i \\ s_i & c_i & 0 & a_i s_i \\ 0 & 0 & 1 & 0 \\ 0 & 0 & 0 & 1 \end{bmatrix} \qquad i = 1, 2, 3. \tag{2.62}$$

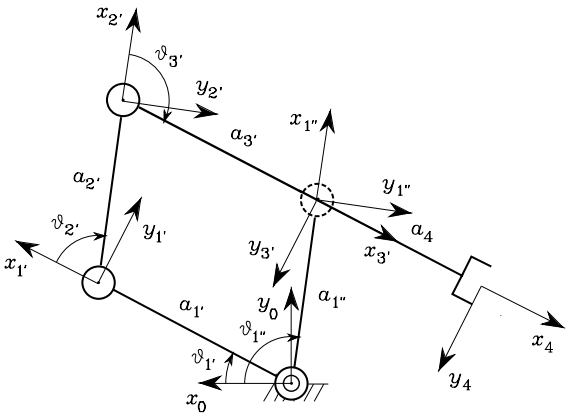

Fig. 2.21. Parallelogram arm

Computation of the direct kinematics function as in (2.50) yields

$$\boldsymbol{T}_3^0(\boldsymbol{q}) = \boldsymbol{A}_1^0\boldsymbol{A}_2^1\boldsymbol{A}_3^2 = \begin{bmatrix} c_{123} & -s_{123} & 0 & a_1c_1 + a_2c_{12} + a_3c_{123} \\ s_{123} & c_{123} & 0 & a_1s_1 + a_2s_{12} + a_3s_{123} \\ 0 & 0 & 1 & 0 \\ 0 & 0 & 0 & 1 \end{bmatrix} \tag{2.63}$$

where $\boldsymbol{q} = [\,\vartheta_1 \quad \vartheta_2 \quad \vartheta_3\,]^T$. Notice that the unit vector $\boldsymbol{z}_3^0$ of Frame 3 is aligned with $\boldsymbol{z}_0 = [\,0 \quad 0 \quad 1\,]^T$, in view of the fact that all revolute joints are parallel to axis z_0. Obviously, $p_z = 0$ and all three joints concur to determine the end-effector position in the plane of the structure. It is worth pointing out that Frame 3 does not coincide with the end-effector frame (Fig. 2.13), since the resulting approach unit vector is aligned with $\boldsymbol{x}_3^0$ and not with $\boldsymbol{z}_3^0$. Thus, assuming that the two frames have the same origin, the constant transformation

$$\boldsymbol{T}_e^3 = \begin{bmatrix} 0 & 0 & 1 & 0 \\ 0 & 1 & 0 & 0 \\ -1 & 0 & 0 & 0 \\ 0 & 0 & 0 & 1 \end{bmatrix}.$$

is needed, having taken $\boldsymbol{n}$ aligned with $\boldsymbol{z}_0$.

2.9.2 Parallelogram Arm

Consider the parallelogram arm in Fig. 2.21. A closed chain occurs where the first two joints connect Link $1'$ and Link $1''$ to Link 0, respectively. Joint 4 was selected as the cut joint, and the link frames have been established accordingly. The DH parameters are specified in Table 2.2, where $a_{1'} = a_{3'}$ and $a_{2'} = a_{1''}$ in view of the parallelogram structure.

Notice that the parameters for Link 4 are all constant. Since the joints are revolute, the homogeneous transformation matrix defined in (2.52) has

Table 2.2. DH parameters for the parallelogram arm

Link	a_i	α_i	d_i	ϑ_i
$1'$	$a_{1'}$	0	0	$\vartheta_{1'}$
$2'$	$a_{2'}$	0	0	$\vartheta_{2'}$
$3'$	$a_{3'}$	0	0	$\vartheta_{3'}$
$1''$	$a_{1''}$	0	0	$\vartheta_{1''}$
4	a_4	0	0	0

the same structure for each joint, i.e., as in (2.62) for Joints $1'$, $2'$, $3'$ and $1''$. Therefore, the coordinate transformations for the two branches of the tree are respectively:

$$\boldsymbol{A}^0_{3'}(\boldsymbol{q}') = \boldsymbol{A}^0_{1'}\boldsymbol{A}^{1'}_{2'}\boldsymbol{A}^{2'}_{3'} = \begin{bmatrix} c_{1'2'3'} & -s_{1'2'3'} & 0 & a_{1'}c_{1'} + a_{2'}c_{1'2'} + a_{3'}c_{1'2'3'} \\ s_{1'2'3'} & c_{1'2'3'} & 0 & a_{1'}s_{1'} + a_{2'}s_{1'2'} + a_{3'}s_{1'2'3'} \\ 0 & 0 & 1 & 0 \\ 0 & 0 & 0 & 1 \end{bmatrix}$$

where $\boldsymbol{q}' = [\,\vartheta_{1'} \quad \vartheta_{2'} \quad \vartheta_{3'}\,]^T$, and

$$\boldsymbol{A}^0_{1''}(q'') = \begin{bmatrix} c_{1''} & -s_{1''} & 0 & a_{1''}c_{1''} \\ s_{1''} & c_{1''} & 0 & a_{1''}s_{1''} \\ 0 & 0 & 1 & 0 \\ 0 & 0 & 0 & 1 \end{bmatrix}$$

where $q'' = \vartheta_{1''}$. To complete, the constant homogeneous transformation for the last link is

$$\boldsymbol{A}^{3'}_4 = \begin{bmatrix} 1 & 0 & 0 & a_4 \\ 0 & 1 & 0 & 0 \\ 0 & 0 & 1 & 0 \\ 0 & 0 & 0 & 1 \end{bmatrix}.$$

With reference to (2.59), the position constraints are ($d_{3'1''} = 0$)

$$\boldsymbol{R}^{3'}_0(\boldsymbol{q}')\left(\boldsymbol{p}^0_{3'}(\boldsymbol{q}') - \boldsymbol{p}^0_{1''}(q'')\right) = \begin{bmatrix} 0 \\ 0 \\ 0 \end{bmatrix}$$

while the orientation constraints are satisfied independently of $\boldsymbol{q}'$ and q''. Since $a_{1'} = a_{3'}$ and $a_{2'} = a_{1''}$, two independent constraints can be extracted, i.e.,

$$\begin{aligned} a_{1'}(c_{1'} + c_{1'2'3'}) + a_{1''}(c_{1'2'} - c_{1''}) &= 0 \\ a_{1'}(s_{1'} + s_{1'2'3'}) + a_{1''}(s_{1'2'} - s_{1''}) &= 0. \end{aligned}$$

In order to satisfy them for any choice of $a_{1'}$ and $a_{1''}$, it must be

$$\begin{aligned} \vartheta_{2'} &= \vartheta_{1''} - \vartheta_{1'} \\ \vartheta_{3'} &= \pi - \vartheta_{2'} = \pi - \vartheta_{1''} + \vartheta_{1'} \end{aligned}$$

Therefore, the vector of joint variables is $\boldsymbol{q} = [\,\vartheta_{1'} \quad \vartheta_{1''}\,]^T$. These joints are natural candidates to be the actuated joints.[10] Substituting the expressions of $\vartheta_{2'}$ and $\vartheta_{3'}$ into the homogeneous transformation $\boldsymbol{A}_{3'}^0$ and computing the direct kinematics function as in (2.61) yields

$$\boldsymbol{T}_4^0(\boldsymbol{q}) = \boldsymbol{A}_{3'}^0(\boldsymbol{q})\boldsymbol{A}_4^{3'} = \begin{bmatrix} -c_{1'} & s_{1'} & 0 & a_{1''}c_{1''} - a_4 c_{1'} \\ -s_{1'} & -c_{1'} & 0 & a_{1''}s_{1''} - a_4 s_{1'} \\ 0 & 0 & 1 & 0 \\ 0 & 0 & 0 & 1 \end{bmatrix}. \tag{2.64}$$

A comparison between (2.64) and (2.49) reveals that the parallelogram arm is kinematically equivalent to a two-link planar arm. The noticeable difference, though, is that the two actuated joints — providing the DOFs of the structure — are located at the base. This will greatly simplify the dynamic model of the structure, as will be seen in Sect. 7.3.3.

2.9.3 Spherical Arm

Consider the spherical arm in Fig. 2.22, where the link frames have been illustrated. Notice that the origin of Frame 0 was located at the intersection of z_0 with z_1 so that $d_1 = 0$; analogously, the origin of Frame 2 was located at the intersection between z_1 and z_2. The DH parameters are specified in Table 2.3.

Table 2.3. DH parameters for the spherical arm

Link	a_i	α_i	d_i	ϑ_i
1	0	$-\pi/2$	0	ϑ_1
2	0	$\pi/2$	d_2	ϑ_2
3	0	0	d_3	0

The homogeneous transformation matrices defined in (2.52) are for the single joints:

$$\boldsymbol{A}_1^0(\vartheta_1) = \begin{bmatrix} c_1 & 0 & -s_1 & 0 \\ s_1 & 0 & c_1 & 0 \\ 0 & -1 & 0 & 0 \\ 0 & 0 & 0 & 1 \end{bmatrix} \qquad \boldsymbol{A}_2^1(\vartheta_2) = \begin{bmatrix} c_2 & 0 & s_2 & 0 \\ s_2 & 0 & -c_2 & 0 \\ 0 & 1 & 0 & d_2 \\ 0 & 0 & 0 & 1 \end{bmatrix}$$

$$\boldsymbol{A}_3^2(d_3) = \begin{bmatrix} 1 & 0 & 0 & 0 \\ 0 & 1 & 0 & 0 \\ 0 & 0 & 1 & d_3 \\ 0 & 0 & 0 & 1 \end{bmatrix}.$$

[10] Notice that it is not possible to solve (2.64) for $\vartheta_{2'}$ and $\vartheta_{3'}$ since they are constrained by the condition $\vartheta_{2'} + \vartheta_{3'} = \pi$.

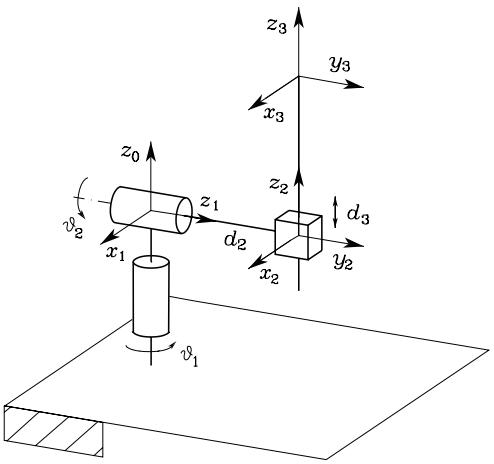

Fig. 2.22. Spherical arm

Computation of the direct kinematics function as in (2.50) yields

$$\boldsymbol{T}_3^0(\boldsymbol{q}) = \boldsymbol{A}_1^0\boldsymbol{A}_2^1\boldsymbol{A}_3^2 = \begin{bmatrix} c_1c_2 & -s_1 & c_1s_2 & c_1s_2d_3 - s_1d_2 \\ s_1c_2 & c_1 & s_1s_2 & s_1s_2d_3 + c_1d_2 \\ -s_2 & 0 & c_2 & c_2d_3 \\ 0 & 0 & 0 & 1 \end{bmatrix} \tag{2.65}$$

where $\boldsymbol{q} = [\,\vartheta_1 \quad \vartheta_2 \quad d_3\,]^T$. Notice that the third joint does not obviously influence the rotation matrix. Further, the orientation of the unit vector $\boldsymbol{y}_3^0$ is uniquely determined by the first joint, since the revolute axis of the second joint z_1 is parallel to axis y_3. Different from the previous structures, in this case Frame 3 can represent an end-effector frame of unit vectors $(\boldsymbol{n}_e, \boldsymbol{s}_e, \boldsymbol{a}_e)$, i.e., $\boldsymbol{T}_e^3 = \boldsymbol{I}_4$.

2.9.4 Anthropomorphic Arm

Consider the anthropomorphic arm in Fig. 2.23. Notice how this arm corresponds to a two-link planar arm with an additional rotation about an axis of the plane. In this respect, the parallelogram arm could be used in lieu of the two-link planar arm, as found in some industrial robots with an anthropomorphic structure.

The link frames have been illustrated in the figure. As for the previous structure, the origin of Frame 0 was chosen at the intersection of z_0 with z_1 ($d_1 = 0$); further, z_1 and z_2 are parallel and the choice of axes x_1 and x_2 was made as for the two-link planar arm. The DH parameters are specified in Table 2.4.

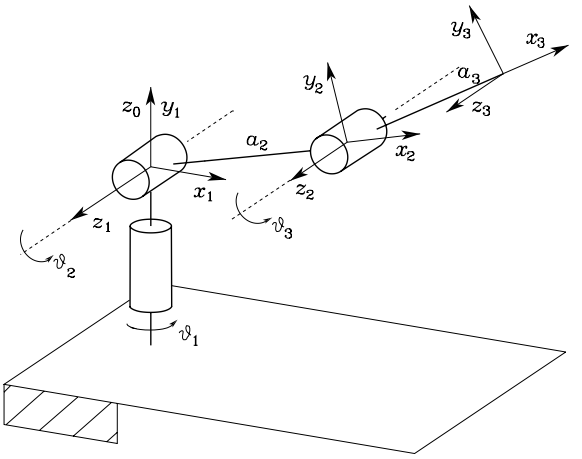

Fig. 2.23. Anthropomorphic arm

Table 2.4. DH parameters for the anthropomorphic arm

Link	a_i	α_i	d_i	ϑ_i
1	0	$\pi/2$	0	ϑ_1
2	a_2	0	0	ϑ_2
3	a_3	0	0	ϑ_3

The homogeneous transformation matrices defined in (2.52) are for the single joints:

$$\boldsymbol{A}_1^0(\vartheta_1) = \begin{bmatrix} c_1 & 0 & s_1 & 0 \\ s_1 & 0 & -c_1 & 0 \\ 0 & 1 & 0 & 0 \\ 0 & 0 & 0 & 1 \end{bmatrix}$$

$$\boldsymbol{A}_i^{i-1}(\vartheta_i) = \begin{bmatrix} c_i & -s_i & 0 & a_i c_i \\ s_i & c_i & 0 & a_i s_i \\ 0 & 0 & 1 & 0 \\ 0 & 0 & 0 & 1 \end{bmatrix} \qquad i = 2, 3.$$

Computation of the direct kinematics function as in (2.50) yields

$$\boldsymbol{T}_3^0(\boldsymbol{q}) = \boldsymbol{A}_1^0 \boldsymbol{A}_2^1 \boldsymbol{A}_3^2 = \begin{bmatrix} c_1 c_{23} & -c_1 s_{23} & s_1 & c_1(a_2 c_2 + a_3 c_{23}) \\ s_1 c_{23} & -s_1 s_{23} & -c_1 & s_1(a_2 c_2 + a_3 c_{23}) \\ s_{23} & c_{23} & 0 & a_2 s_2 + a_3 s_{23} \\ 0 & 0 & 0 & 1 \end{bmatrix} \tag{2.66}$$

where $\boldsymbol{q} = [\,\vartheta_1 \quad \vartheta_2 \quad \vartheta_3\,]^T$. Since z_3 is aligned with z_2, Frame 3 does not coincide with a possible end-effector frame as in Fig. 2.13, and a proper constant transformation would be needed.

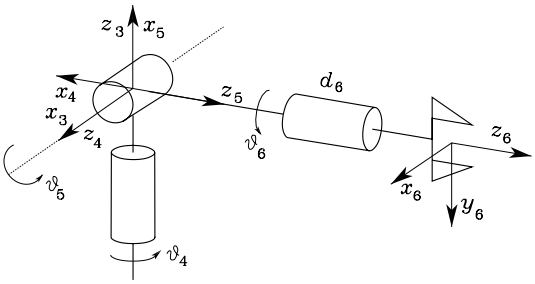

Fig. 2.24. Spherical wrist

2.9.5 Spherical Wrist

Consider a particular type of structure consisting just of the wrist of Fig. 2.24. Joint variables were numbered progressively starting from 4, since such a wrist is typically thought of as mounted on a three-DOF arm of a six-DOF manipulator. It is worth noticing that the wrist is spherical since all revolute axes intersect at a single point. Once z_3, z_4, z_5 have been established, and x_3 has been chosen, there is an indeterminacy on the directions of x_4 and x_5. With reference to the frames indicated in Fig. 2.24, the DH parameters are specified in Table 2.5.

Table 2.5. DH parameters for the spherical wrist

Link	a_i	α_i	d_i	ϑ_i
4	0	$-\pi/2$	0	ϑ_4
5	0	$\pi/2$	0	ϑ_5
6	0	0	d_6	ϑ_6

The homogeneous transformation matrices defined in (2.52) are for the single joints:

$$\boldsymbol{A}_4^3(\vartheta_4) = \begin{bmatrix} c_4 & 0 & -s_4 & 0 \\ s_4 & 0 & c_4 & 0 \\ 0 & -1 & 0 & 0 \\ 0 & 0 & 0 & 1 \end{bmatrix} \qquad \boldsymbol{A}_5^4(\vartheta_5) = \begin{bmatrix} c_5 & 0 & s_5 & 0 \\ s_5 & 0 & -c_5 & 0 \\ 0 & 1 & 0 & 0 \\ 0 & 0 & 0 & 1 \end{bmatrix}$$

$$\boldsymbol{A}_6^5(\vartheta_6) = \begin{bmatrix} c_6 & -s_6 & 0 & 0 \\ s_6 & c_6 & 0 & 0 \\ 0 & 0 & 1 & d_6 \\ 0 & 0 & 0 & 1 \end{bmatrix}.$$

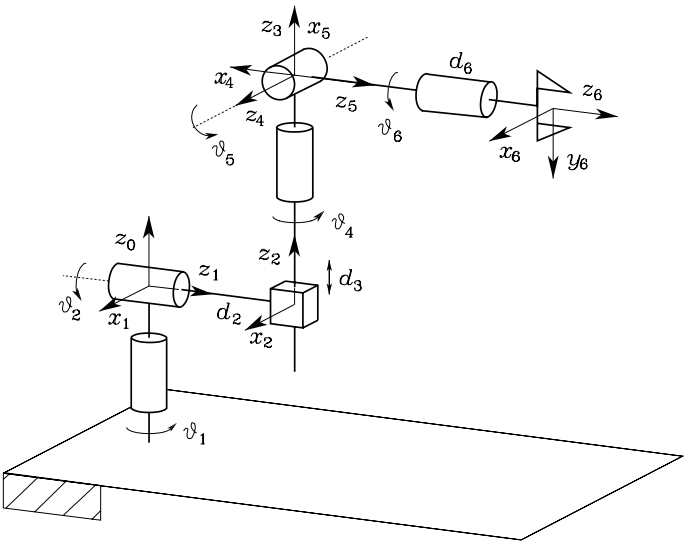

Fig. 2.25. Stanford manipulator

Computation of the direct kinematics function as in (2.50) yields

$$\boldsymbol{T}_6^3(\boldsymbol{q}) = \boldsymbol{A}_4^3\boldsymbol{A}_5^4\boldsymbol{A}_6^5 = \begin{bmatrix} c_4c_5c_6 - s_4s_6 & -c_4c_5s_6 - s_4c_6 & c_4s_5 & c_4s_5d_6 \\ s_4c_5c_6 + c_4s_6 & -s_4c_5s_6 + c_4c_6 & s_4s_5 & s_4s_5d_6 \\ -s_5c_6 & s_5s_6 & c_5 & c_5d_6 \\ 0 & 0 & 0 & 1 \end{bmatrix} \tag{2.67}$$

where $\boldsymbol{q} = [\,\vartheta_4 \quad \vartheta_5 \quad \vartheta_6\,]^T$. Notice that, as a consequence of the choice made for the coordinate frames, the block matrix $\boldsymbol{R}_6^3$ that can be extracted from $\boldsymbol{T}_6^3$ coincides with the rotation matrix of Euler angles (2.18) previously derived, that is, ϑ_4, ϑ_5, ϑ_6 constitute the set of ZYZ angles with respect to the reference frame O_3–$x_3y_3z_3$. Moreover, the unit vectors of Frame 6 coincide with the unit vectors of a possible end-effector frame according to Fig. 2.13.

2.9.6 Stanford Manipulator

The so-called Stanford manipulator is composed of a spherical arm and a spherical wrist (Fig. 2.25). Since Frame 3 of the spherical arm coincides with Frame 3 of the spherical wrist, the direct kinematics function can be obtained via simple composition of the transformation matrices (2.65), (2.67) of the previous examples, i.e.,

$$\boldsymbol{T}_6^0 = \boldsymbol{T}_3^0\boldsymbol{T}_6^3 = \begin{bmatrix} \boldsymbol{n}^0 & \boldsymbol{s}^0 & \boldsymbol{a}^0 & \boldsymbol{p}^0 \\ 0 & 0 & 0 & 1 \end{bmatrix}.$$

Carrying out the products yields

$$\boldsymbol{p}_6^0 = \begin{bmatrix} c_1 s_2 d_3 - s_1 d_2 + \big(c_1(c_2 c_4 s_5 + s_2 c_5) - s_1 s_4 s_5\big) d_6 \\ s_1 s_2 d_3 + c_1 d_2 + \big(s_1(c_2 c_4 s_5 + s_2 c_5) + c_1 s_4 s_5\big) d_6 \\ c_2 d_3 + (-s_2 c_4 s_5 + c_2 c_5) d_6 \end{bmatrix} \tag{2.68}$$

for the end-effector position, and

$$\begin{aligned} \boldsymbol{n}_6^0 &= \begin{bmatrix} c_1\big(c_2(c_4 c_5 c_6 - s_4 s_6) - s_2 s_5 c_6\big) - s_1(s_4 c_5 c_6 + c_4 s_6) \\ s_1\big(c_2(c_4 c_5 c_6 - s_4 s_6) - s_2 s_5 c_6\big) + c_1(s_4 c_5 c_6 + c_4 s_6) \\ -s_2(c_4 c_5 c_6 - s_4 s_6) - c_2 s_5 c_6 \end{bmatrix} \\ \boldsymbol{s}_6^0 &= \begin{bmatrix} c_1\big(-c_2(c_4 c_5 s_6 + s_4 c_6) + s_2 s_5 s_6\big) - s_1(-s_4 c_5 s_6 + c_4 c_6) \\ s_1\big(-c_2(c_4 c_5 s_6 + s_4 c_6) + s_2 s_5 s_6\big) + c_1(-s_4 c_5 s_6 + c_4 c_6) \\ s_2(c_4 c_5 s_6 + s_4 c_6) + c_2 s_5 s_6 \end{bmatrix} \\ \boldsymbol{a}_6^0 &= \begin{bmatrix} c_1(c_2 c_4 s_5 + s_2 c_5) - s_1 s_4 s_5 \\ s_1(c_2 c_4 s_5 + s_2 c_5) + c_1 s_4 s_5 \\ -s_2 c_4 s_5 + c_2 c_5 \end{bmatrix} \end{aligned} \tag{2.69}$$

for the end-effector orientation.

A comparison of the vector $\boldsymbol{p}_6^0$ in (2.68) with the vector $\boldsymbol{p}_3^0$ in (2.65) relative to the sole spherical arm reveals the presence of additional contributions due to the choice of the origin of the end-effector frame at a distance d_6 from the origin of Frame 3 along the direction of $\boldsymbol{a}_6^0$. In other words, if it were $d_6 = 0$, the position vector would be the same. This feature is of fundamental importance for the solution of the inverse kinematics for this manipulator, as will be seen later.

2.9.7 Anthropomorphic Arm with Spherical Wrist

A comparison between Fig. 2.23 and Fig. 2.24 reveals that the direct kinematics function cannot be obtained by multiplying the transformation matrices $\boldsymbol{T}_3^0$ and $\boldsymbol{T}_6^3$, since Frame 3 of the anthropomorphic arm cannot coincide with Frame 3 of the spherical wrist.

Direct kinematics of the entire structure can be obtained in two ways. One consists of interposing a constant transformation matrix between $\boldsymbol{T}_3^0$ and $\boldsymbol{T}_6^3$ which allows the alignment of the two frames. The other refers to the Denavit–Hartenberg operating procedure with the frame assignment for the entire structure illustrated in Fig. 2.26. The DH parameters are specified in Table 2.6.

Since Rows 3 and 4 differ from the corresponding rows of the tables for the two single structures, the relative homogeneous transformation matrices $\boldsymbol{A}_3^2$ and $\boldsymbol{A}_4^3$ have to be modified into

$$\boldsymbol{A}_3^2(\vartheta_3) = \begin{bmatrix} c_3 & 0 & s_3 & 0 \\ s_3 & 0 & -c_3 & 0 \\ 0 & 1 & 0 & 0 \\ 0 & 0 & 0 & 1 \end{bmatrix} \qquad \boldsymbol{A}_4^3(\vartheta_4) = \begin{bmatrix} c_4 & 0 & -s_4 & 0 \\ s_4 & 0 & c_4 & 0 \\ 0 & -1 & 0 & d_4 \\ 0 & 0 & 0 & 1 \end{bmatrix}$$

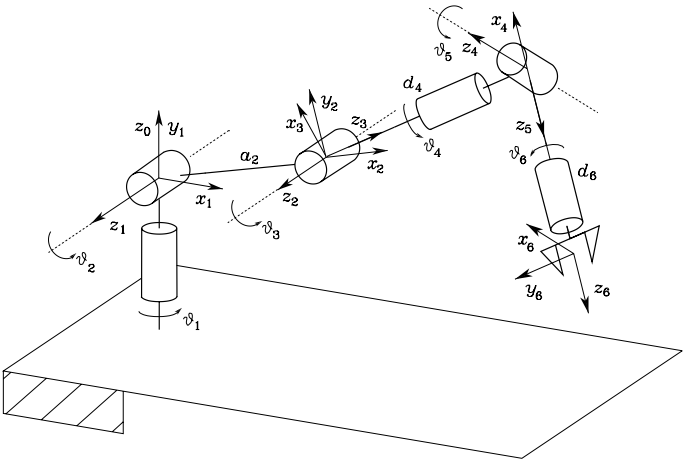

Fig. 2.26. Anthropomorphic arm with spherical wrist

Table 2.6. DH parameters for the anthropomorphic arm with spherical wrist

Link	a_i	α_i	d_i	ϑ_i
1	0	$\pi/2$	0	ϑ_1
2	a_2	0	0	ϑ_2
3	0	$\pi/2$	0	ϑ_3
4	0	$-\pi/2$	d_4	ϑ_4
5	0	$\pi/2$	0	ϑ_5
6	0	0	d_6	ϑ_6

while the other transformation matrices remain the same. Computation of the direct kinematics function leads to expressing the position and orientation of the end-effector frame as:

$$\boldsymbol{p}_6^0 = \begin{bmatrix} a_2c_1c_2 + d_4c_1s_{23} + d_6\big(c_1(c_{23}c_4s_5 + s_{23}c_5) + s_1s_4s_5\big) \\ a_2s_1c_2 + d_4s_1s_{23} + d_6\big(s_1(c_{23}c_4s_5 + s_{23}c_5) - c_1s_4s_5\big) \\ a_2s_2 - d_4c_{23} + d_6(s_{23}c_4s_5 - c_{23}c_5) \end{bmatrix} \tag{2.70}$$

and

$$\begin{aligned} \boldsymbol{n}_6^0 &= \begin{bmatrix} c_1\big(c_{23}(c_4c_5c_6 - s_4s_6) - s_{23}s_5c_6\big) + s_1(s_4c_5c_6 + c_4s_6) \\ s_1\big(c_{23}(c_4c_5c_6 - s_4s_6) - s_{23}s_5c_6\big) - c_1(s_4c_5c_6 + c_4s_6) \\ s_{23}(c_4c_5c_6 - s_4s_6) + c_{23}s_5c_6 \end{bmatrix} \\ \boldsymbol{s}_6^0 &= \begin{bmatrix} c_1\big(-c_{23}(c_4c_5s_6 + s_4c_6) + s_{23}s_5s_6\big) + s_1(-s_4c_5s_6 + c_4c_6) \\ s_1\big(-c_{23}(c_4c_5s_6 + s_4c_6) + s_{23}s_5s_6\big) - c_1(-s_4c_5s_6 + c_4c_6) \\ -s_{23}(c_4c_5s_6 + s_4c_6) - c_{23}s_5s_6 \end{bmatrix} \\ \boldsymbol{a}_6^0 &= \begin{bmatrix} c_1(c_{23}c_4s_5 + s_{23}c_5) + s_1s_4s_5 \\ s_1(c_{23}c_4s_5 + s_{23}c_5) - c_1s_4s_5 \\ s_{23}c_4s_5 - c_{23}c_5 \end{bmatrix}. \end{aligned} \tag{2.71}$$

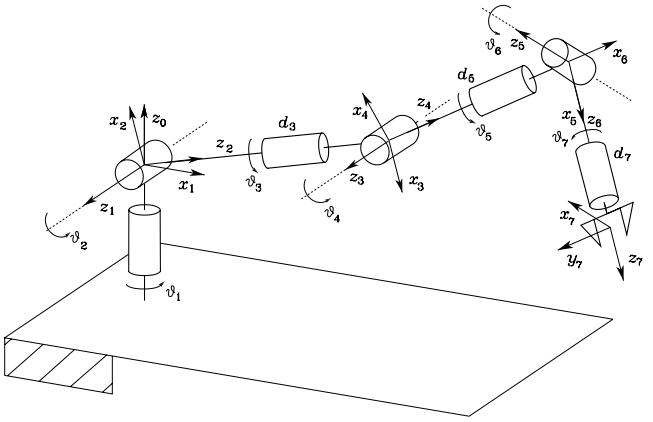

Fig. 2.27. DLR manipulator

By setting $d_6 = 0$, the position of the wrist axes intersection is obtained. In that case, the vector $\boldsymbol{p}^0$ in (2.70) corresponds to the vector $\boldsymbol{p}_3^0$ for the sole anthropomorphic arm in (2.66), because d_4 gives the length of the forearm (a_3) and axis x_3 in Fig. 2.26 is rotated by $\pi/2$ with respect to axis x_3 in Fig. 2.23.

2.9.8 DLR Manipulator

Consider the DLR manipulator, whose development is at the basis of the realization of the robot in Fig. 1.30; it is characterized by seven DOFs and as such it is inherently redundant. This manipulator has two possible configurations for the outer three joints (wrist). With reference to a spherical wrist similar to that introduced in Sect. 2.9.5, the resulting kinematic structure is illustrated in Fig. 2.27, where the frames attached to the links are evidenced.

As in the case of the spherical arm, notice that the origin of Frame 0 has been chosen so as to zero d_1. The DH parameters are specified in Table 2.7.

Table 2.7. DH parameters for the DLR manipulator

Link	a_i	α_i	d_i	ϑ_i
1	0	$\pi/2$	0	ϑ_1
2	0	$\pi/2$	0	ϑ_2
3	0	$\pi/2$	d_3	ϑ_3
4	0	$\pi/2$	0	ϑ_4
5	0	$\pi/2$	d_5	ϑ_5
6	0	$\pi/2$	0	ϑ_6
7	0	0	d_7	ϑ_7

The generic homogeneous transformation matrix defined in (2.52) is ($\alpha_i = \pi/2$)

$$\boldsymbol{A}_i^{i-1} = \begin{bmatrix} c_i & 0 & s_i & 0 \\ s_i & 0 & -c_i & 0 \\ 0 & 1 & 0 & d_i \\ 0 & 0 & 0 & 1 \end{bmatrix} \qquad i = 1, \ldots, 6 \tag{2.72}$$

while, since $\alpha_7 = 0$, it is

$$\boldsymbol{A}_7^6 = \begin{bmatrix} c_7 & -s_7 & 0 & 0 \\ s_7 & c_7 & 0 & 0 \\ 0 & 0 & 1 & d_7 \\ 0 & 0 & 0 & 1 \end{bmatrix}. \tag{2.73}$$

The direct kinematics function, computed as in (2.50), leads to the following expressions for the end-effector frame

$$\boldsymbol{p}_7^0 = \begin{bmatrix} d_3 x_{d_3} + d_5 x_{d_5} + d_7 x_{d_7} \\ d_3 y_{d_3} + d_5 y_{d_5} + d_7 y_{d_7} \\ d_3 z_{d_3} + d_5 z_{d_5} + d_7 z_{d_7} \end{bmatrix} \tag{2.74}$$

with

$$\begin{aligned} x_{d_3} &= c_1 s_2 \\ x_{d_5} &= c_1(c_2 c_3 s_4 - s_2 c_4) + s_1 s_3 s_4 \\ x_{d_7} &= c_1(c_2 k_1 + s_2 k_2) + s_1 k_3 \\ y_{d_3} &= s_1 s_2 \\ y_{d_5} &= s_1(c_2 c_3 s_4 - s_2 c_4) - c_1 s_3 s_4 \\ y_{d_7} &= s_1(c_2 k_1 + s_2 k_2) - c_1 k_3 \\ z_{d_3} &= -c_2 \\ z_{d_5} &= c_2 c_4 + s_2 c_3 s_4 \\ z_{d_7} &= s_2(c_3(c_4 c_5 s_6 - s_4 c_6) + s_3 s_5 s_6) - c_2 k_2, \end{aligned}$$

where

$$\begin{aligned} k_1 &= c_3(c_4 c_5 s_6 - s_4 c_6) + s_3 s_5 s_6 \\ k_2 &= s_4 c_5 s_6 + c_4 c_6 \\ k_3 &= s_3(c_4 c_5 s_6 - s_4 c_6) - c_3 s_5 s_6. \end{aligned}$$

Furthermore, the end-effector frame orientation can be derived as

$$\boldsymbol{n}_7^0 = \begin{bmatrix} ((x_a c_5 + x_c s_5) c_6 + x_b s_6) c_7 + (x_a s_5 - x_c c_5) s_7 \\ ((y_a c_5 + y_c s_5) c_6 + y_b s_6) c_7 + (y_a s_5 - y_c c_5) s_7 \\ (z_a c_6 + z_c s_6) c_7 + z_b s_7 \end{bmatrix}$$

$$\boldsymbol{s}_7^0 = \begin{bmatrix} -((x_a c_5 + x_c s_5)c_6 + x_b s_6)s_7 + (x_a s_5 - x_c c_5)c_7 \\ -((y_a c_5 + y_c s_5)c_6 + y_b s_6)s_7 + (y_a s_5 - y_c c_5)c_7 \\ -(z_a c_6 + z_c s_6)s_7 + z_b c_7 \end{bmatrix} \qquad (2.75)$$

$$\boldsymbol{a}_7^0 = \begin{bmatrix} (x_a c_5 + x_c s_5)s_6 - x_b c_6 \\ (y_a c_5 + y_c s_5)s_6 - y_b c_6 \\ z_a s_6 - z_c c_6 \end{bmatrix},$$

where

$$\begin{aligned} x_a &= (c_1 c_2 c_3 + s_1 s_3)c_4 + c_1 s_2 s_4 \\ x_b &= (c_1 c_2 c_3 + s_1 s_3)s_4 - c_1 s_2 c_4 \\ x_c &= c_1 c_2 s_3 - s_1 c_3 \\ y_a &= (s_1 c_2 c_3 - c_1 s_3)c_4 + s_1 s_2 s_4 \\ y_b &= (s_1 c_2 c_3 - c_1 s_3)s_4 - s_1 s_2 c_4 \\ y_c &= s_1 c_2 s_3 + c_1 c_3 \\ z_a &= (s_2 c_3 c_4 - c_2 s_4)c_5 + s_2 s_3 s_5 \\ z_b &= (s_2 c_3 c_4 - c_2 s_4)s_5 - s_2 s_3 c_5 \\ z_c &= s_2 c_3 s_4 + c_2 c_4. \end{aligned} \qquad (2.76)$$

As in the case of the anthropomorphic arm with spherical wrist, it occurs that Frame 4 cannot coincide with the base frame of the wrist.

Finally, consider the possibility to mount a different type of spherical wrist, where Joint 7 is so that $\alpha_7 = \pi/2$. In such a case, the computation of the direct kinematics function changes, since the seventh row of the kinematic parameters table changes. In particular, notice that, since $d_7 = 0$, $a_7 \neq 0$, then

$$\boldsymbol{A}_7^6 = \begin{bmatrix} c_7 & 0 & s_7 & a_7 c_7 \\ s_7 & 0 & -c_7 & a_7 s_7 \\ 0 & 0 & 1 & 0 \\ 0 & 0 & 0 & 1 \end{bmatrix}. \qquad (2.77)$$

It follows, however, that Frame 7 does not coincide with the end-effector frame, as already discussed for the three-link planar arm, since the approach unit vector $\boldsymbol{a}_7^0$ is aligned with x_7.

2.9.9 Humanoid Manipulator

The term humanoid refers to a robot showing a kinematic structure similar to that of the human body. It is commonly thought that the most relevant feature of humanoid robots is biped locomotion. However, in detail, a humanoid manipulator refers to an articulated structure with a kinematics analogous to

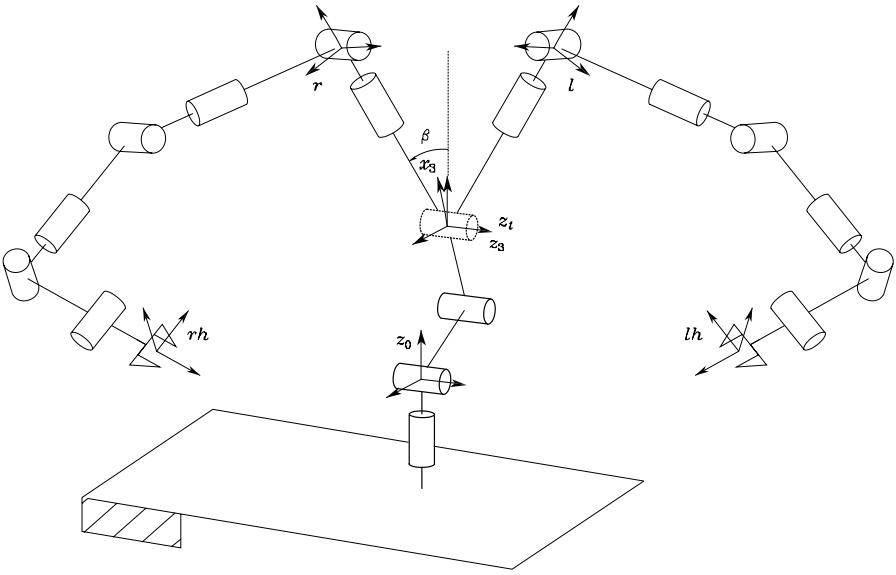

Fig. 2.28. Humanoid manipulator

that of the human body upper part: torso, arms, end-effectors similar to human hands and a 'head' which, eventually, includes an artificial vision system — see Chap. 10.

For the humanoid manipulator in Fig. 1.33, it is worth noticing the presence of two end-effectors (where the 'hands' are mounted), while the arms consist of two DLR manipulators, introduced in the previous section, each with seven DOFs. In particular, consider the configuration where the last joint is so that $\alpha_7 = \pi/2$.

To simplify, the kinematic structure allowing the articulation of the robot's head in Fig. 1.33. The torso can be modelled as an anthropomorphic arm (three DOFs), for a total of seventeen DOFs.

Further, a connecting device exists between the end-effector of the anthropomorphic torso and the base frames of the two manipulators. Such device permits keeping the 'chest' of the humanoid manipulator always orthogonal to the ground. With reference to Fig. 2.28, this device is represented by a further joint, located at the end of the torso. Hence, the corresponding parameter ϑ_4 does not constitute a DOF, yet it varies so as to compensate Joints 2 and 3 rotations of the anthropomorphic torso.

To compute the direct kinematics function, it is possible to resort to a DH parameters table for each of the two tree kinematic structures, which can be identified from the base of the manipulator to each of the two end-effectors. Similarly to the case of mounting a spherical wrist onto an anthropomorphic arm, this implies the change of some rows of the transformation matrices of

those manipulators, described in the previous sections, constituting the torso and the arms.

Alternatively, it is possible to consider intermediate transformation matrices between the relevant structures. In detail, as illustrated in Fig. 2.28, if t denotes the frame attached to the torso, r and l the base frames, respectively, of the right arm and the left arm, and rh and lh the frames attached to the two hands (end-effectors), it is possible to compute for the right arm and the left arm, respectively:

$$\boldsymbol{T}_{rh}^{0} = \boldsymbol{T}_{3}^{0}\,\boldsymbol{T}_{t}^{3}\,\boldsymbol{T}_{r}^{t}\boldsymbol{T}_{rh}^{r} \tag{2.78}$$

$$\boldsymbol{T}_{lh}^{0} = \boldsymbol{T}_{3}^{0}\,\boldsymbol{T}_{t}^{3}\,\boldsymbol{T}_{l}^{t}\boldsymbol{T}_{lh}^{l} \tag{2.79}$$

where the matrix $\boldsymbol{T}_{t}^{3}$ describes the transformation imposed by the motion of Joint 4 (dashed line in Fig. 2.28), located at the end-effector of the torso. Frame 4 coincides with Frame t in Fig. 2.27. In view of the property of parameter ϑ_4, it is $\vartheta_4 = -\vartheta_2 - \vartheta_3$, and thus

$$\boldsymbol{T}_{t}^{3} = \begin{bmatrix} c_{23} & s_{23} & 0 & 0 \\ -s_{23} & c_{23} & 0 & 0 \\ 0 & 0 & 1 & 0 \\ 0 & 0 & 0 & 1 \end{bmatrix}.$$

The matrix $\boldsymbol{T}_{3}^{0}$ is given by (2.66), whereas the matrices $\boldsymbol{T}_{r}^{t}$ and $\boldsymbol{T}_{l}^{t}$ relating the torso end-effector frame to the base frames of the two manipulators have constant values. With reference to Fig. 2.28, the elements of these matrices depend on the angle β and on the distances between the origin of Frame t and the origins of Frames r and l. Finally, the expressions of the matrices $\boldsymbol{T}_{rh}^{r}$ and $\boldsymbol{T}_{lh}^{l}$ must be computed by considering the change in the seventh row of the DH parameters table of the DLR manipulator, so as to account for the different kinematic structure of the wrist (see Problem 2.14).

2.10 Joint Space and Operational Space

As described in the previous sections, the direct kinematics equation of a manipulator allows the position and orientation of the end-effector frame to be expressed as a function of the joint variables with respect to the base frame.

If a task is to be specified for the end-effector, it is necessary to assign the end-effector position and orientation, eventually as a function of time (trajectory). This is quite easy for the position. On the other hand, specifying the orientation through the unit vector triplet $(\boldsymbol{n}_e, \boldsymbol{s}_e, \boldsymbol{a}_e)$[11] is quite difficult, since their nine components must be guaranteed to satisfy the orthonormality constraints imposed by (2.4) at each time instant. This problem will be resumed in Chap. 4.

[11] To simplify, the indication of the reference frame in the superscript is omitted.

The problem of describing end-effector orientation admits a natural solution if one of the above minimal representations is adopted. In this case, indeed, a motion trajectory can be assigned to the set of angles chosen to represent orientation.

Therefore, the position can be given by a minimal number of coordinates with regard to the geometry of the structure, and the orientation can be specified in terms of a minimal representation (Euler angles) describing the rotation of the end-effector frame with respect to the base frame. In this way, it is possible to describe the end-effector pose by means of the $(m \times 1)$ vector, with $m \leq n$,

$$\boldsymbol{x}_e = \begin{bmatrix} \boldsymbol{p}_e \\ \boldsymbol{\phi}_e \end{bmatrix} \tag{2.80}$$

where $\boldsymbol{p}_e$ describes the end-effector position and $\boldsymbol{\phi}_e$ its orientation.

This representation of position and orientation allows the description of an end-effector task in terms of a number of inherently independent parameters. The vector $\boldsymbol{x}_e$ is defined in the space in which the manipulator task is specified; hence, this space is typically called *operational space*. On the other hand, the *joint space* (configuration space) denotes the space in which the $(n \times 1)$ vector of joint variables

$$\boldsymbol{q} = \begin{bmatrix} q_1 \\ \vdots \\ q_n \end{bmatrix}, \tag{2.81}$$

is defined; it is $q_i = \vartheta_i$ for a revolute joint and $q_i = d_i$ for a prismatic joint. Accounting for the dependence of position and orientation from the joint variables, the direct kinematics equation can be written in a form other than (2.50), i.e.,

$$\boldsymbol{x}_e = \boldsymbol{k}(\boldsymbol{q}). \tag{2.82}$$

The $(m \times 1)$ vector function $\boldsymbol{k}(\cdot)$ — nonlinear in general — allows computation of the operational space variables from the knowledge of the joint space variables.

It is worth noticing that the dependence of the orientation components of the function $\boldsymbol{k}(\boldsymbol{q})$ in (2.82) on the joint variables is not easy to express except for simple cases. In fact, in the most general case of a six-dimensional operational space ($m = 6$), the computation of the three components of the function $\boldsymbol{\phi}_e(\boldsymbol{q})$ cannot be performed in closed form but goes through the computation of the elements of the rotation matrix, i.e., $\boldsymbol{n}_e(\boldsymbol{q})$, $\boldsymbol{s}_e(\boldsymbol{q})$, $\boldsymbol{a}_e(\boldsymbol{q})$. The equations that allow the determination of the Euler angles from the triplet of unit vectors $\boldsymbol{n}_e$, $\boldsymbol{s}_e$, $\boldsymbol{a}_e$ were given in Sect. 2.4.

Example 2.5

Consider again the three-link planar arm in Fig. 2.20. The geometry of the structure suggests that the end-effector position is determined by the two coordinates p_x and p_y, while its orientation is determined by the angle ϕ formed by the end-effector with the axis x_0. Expressing these operational variables as a function of the joint variables, the two position coordinates are given by the first two elements of the fourth column of the homogeneous transformation matrix (2.63), while the orientation angle is simply given by the sum of joint variables. In sum, the direct kinematics equation can be written in the form

$$\boldsymbol{x}_e = \begin{bmatrix} p_x \\ p_y \\ \phi \end{bmatrix} = \boldsymbol{k}(\boldsymbol{q}) = \begin{bmatrix} a_1 c_1 + a_2 c_{12} + a_3 c_{123} \\ a_1 s_1 + a_2 s_{12} + a_3 s_{123} \\ \vartheta_1 + \vartheta_2 + \vartheta_3 \end{bmatrix}. \tag{2.83}$$

This expression shows that three joint space variables allow specification of at most three independent operational space variables. On the other hand, if orientation is of no concern, it is $\boldsymbol{x}_e = [\, p_x \quad p_y \,]^T$ and there is *kinematic redundancy* of DOFs with respect to a pure positioning end-effector task; this concept will be dealt with in detail afterwards.

2.10.1 Workspace

With reference to the operational space, an index of robot performance is the so-called *workspace*; this is the region described by the origin of the end-effector frame when all the manipulator joints execute all possible motions. It is often customary to distinguish between *reachable* workspace and *dexterous* workspace. The latter is the region that the origin of the end-effector frame can describe while attaining different orientations, while the former is the region that the origin of the end-effector frame can reach with at least one orientation. Obviously, the dexterous workspace is a subspace of the reachable workspace. A manipulator with less than six DOFs cannot take any arbitrary position and orientation in space.

The workspace is characterized by the manipulator geometry and the mechanical joint limits. For an n-DOF manipulator, the reachable workspace is the geometric locus of the points that can be achieved by considering the direct kinematics equation for the sole position part, i.e.,

$$\boldsymbol{p}_e = \boldsymbol{p}_e(\boldsymbol{q}) \qquad q_{im} \leq q_i \leq q_{iM} \quad i = 1, \ldots, n,$$

where q_{im} (q_{iM}) denotes the minimum (maximum) limit at Joint i. This volume is finite, closed, connected — $\boldsymbol{p}_e(\boldsymbol{q})$ is a continuous function — and thus is defined by its bordering surface. Since the joints are revolute or prismatic, it is easy to recognize that this surface is constituted by surface elements of planar, spherical, toroidal and cylindrical type. The manipulator workspace

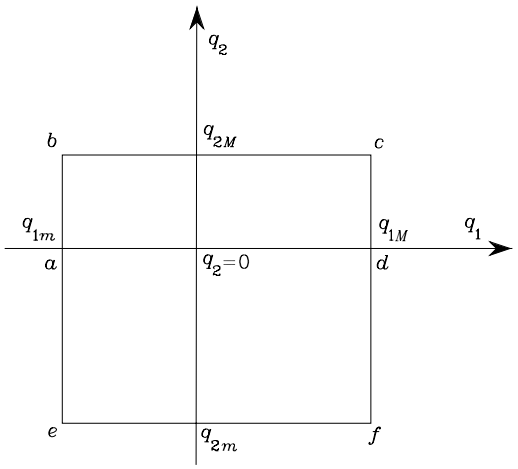

Fig. 2.29. Region of admissible configurations for a two-link arm

(without end-effector) is reported in the data sheet given by the robot manufacturer in terms of a top view and a side view. It represents a basic element to evaluate robot performance for a desired application.

Example 2.6

Consider the simple two-link planar arm. If the mechanical joint limits are known, the arm can attain all the joint space configurations corresponding to the points in the rectangle in Fig. 2.29.

The reachable workspace can be derived via a graphical construction of the image of the rectangle perimeter in the plane of the arm. To this purpose, it is worth considering the images of the segments ab, bc, cd, da, ae, ef, fd. Along the segments ab, bc, cd, ae, ef, fd a loss of mobility occurs due to a joint limit; a loss of mobility occurs also along the segment ad because the arm and forearm are aligned.[12] Further, a change of the arm posture occurs at points a and d: for $q_2 > 0$ the *elbow-down* posture is obtained, while for $q_2 < 0$ the arm is in the *elbow-up* posture.

In the plane of the arm, start drawing the arm in configuration A corresponding to q_{1m} and $q_2 = 0$ (a); then, the segment ab describing motion from $q_2 = 0$ to q_{2M} generates the arc AB; the subsequent arcs BC, CD, DA, AE, EF, FD are generated in a similar way (Fig. 2.30). The external contour of the area $CDAEFHC$ delimits the requested workspace. Further, the area $BCDAB$ is relative to elbow-down postures while the area $DAEFD$ is relative to elbow-up postures; hence, the points in the area $BADHB$ are reachable by the end-effector with both postures.

---

[12] In the following chapter, it will be seen that this configuration characterizes a kinematic *singularity* of the arm.

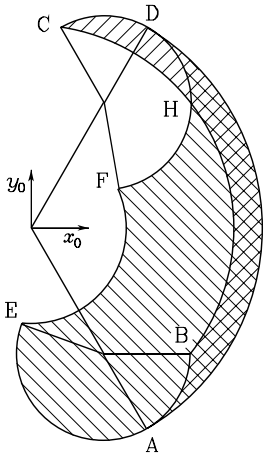

Fig. 2.30. Workspace of a two-link planar arm

In a real manipulator, for a given set of joint variables, the actual values of the operational space variables deviate from those computed via direct kinematics. The direct kinematics equation has indeed a dependence from the DH parameters which is not explicit in (2.82). If the mechanical dimensions of the structure differ from the corresponding parameter of the table because of mechanical tolerances, a deviation arises between the position reached in the assigned posture and the position computed via direct kinematics. Such a deviation is defined *accuracy*; this parameter attains typical values below one millimeter and depends on the structure as well as on manipulator dimensions. Accuracy varies with the end-effector position in the workspace and it is a relevant parameter when robot programming oriented environments are adopted, as will be seen in Chap. 6.

Another parameter that is usually listed in the performance data sheet of an industrial robot is *repeatability* which gives a measure of the manipulator's ability to return to a previously reached position; this parameter is relevant for programming an industrial robot by the teaching–by–showing technique which will be presented in Chap. 6. Repeatability depends not only on the characteristics of the mechanical structure but also on the transducers and controller; it is expressed in metric units and is typically smaller than accuracy. For instance, for a manipulator with a maximum reach of 1.5 m, accuracy varies from 0.2 to 1 mm in the workspace, while repeatability varies from 0.02 to 0.2 mm.

2.10.2 Kinematic Redundancy

A manipulator is termed *kinematically redundant* when it has a number of DOFs which is greater than the number of variables that are necessary to

describe a given task. With reference to the above-defined spaces, a manipulator is intrinsically redundant when the dimension of the operational space is smaller than the dimension of the joint space ($m < n$). Redundancy is, anyhow, a concept *relative* to the task assigned to the manipulator; a manipulator can be redundant with respect to a task and nonredundant with respect to another. Even in the case of $m = n$, a manipulator can be functionally redundant when only a number of r components of operational space are of concern for the specific task, with $r < m$.

Consider again the three-DOF planar arm of Sect. 2.9.1. If only the end-effector position (in the plane) is specified, that structure presents a functional redundancy ($n = m = 3$, $r = 2$); this is lost when also the end-effector orientation in the plane is specified ($n = m = r = 3$). On the other hand, a four-DOF planar arm is intrinsically redundant ($n = 4$, $m = 3$).

Yet, take the typical industrial robot with six DOFs; such manipulator is not intrinsically redundant ($n = m = 6$), but it can become functionally redundant with regard to the task to execute. Thus, for instance, in a laser-cutting task a functional redundancy will occur since the end-effector rotation about the approach direction is irrelevant to completion of the task ($r = 5$).

At this point, a question should arise spontaneously: Why to intentionally utilize a redundant manipulator? The answer is to recognize that redundancy can provide the manipulator with dexterity and versatility in its motion. The typical example is constituted by the human arm that has *seven* DOFs: three in the shoulder, one in the elbow and three in the wrist, without considering the DOFs in the fingers. This manipulator is intrinsically redundant; in fact, if the base and the hand position and orientation are both fixed — requiring six DOFs — the elbow can be moved, thanks to the additional available DOF. Then, for instance, it is possible to avoid obstacles in the workspace. Further, if a joint of a redundant manipulator reaches its mechanical limit, there might be other joints that allow execution of the prescribed end-effector motion.

A formal treatment of redundancy will be presented in the following chapter.

2.11 Kinematic Calibration

The Denavit–Hartenberg parameters for direct kinematics need to be computed as precisely as possible in order to improve manipulator accuracy. *Kinematic calibration* techniques are devoted to finding accurate estimates of DH parameters from a series of measurements on the manipulator's end-effector pose. Hence, they do not allow direct measurement of the geometric parameters of the structure.

Consider the direct kinematics equation in (2.82) which can be rewritten by emphasizing the dependence of the operational space variables on the fixed DH parameters, besides the joint variables. Let $\boldsymbol{a} = [\, a_1 \quad \dots \quad a_n \,]^T$, $\boldsymbol{\alpha} =$

$[\,\alpha_1 \quad \dots \quad \alpha_n\,]^T$, $\boldsymbol{d} = [\,d_1 \quad \dots \quad d_n\,]^T$, and $\boldsymbol{\vartheta} = [\,\theta_1 \quad \dots \quad \theta_n\,]^T$ denote the vectors of DH parameters for the whole structure; then (2.82) becomes

$$\boldsymbol{x}_e = \boldsymbol{k}(\boldsymbol{a}, \boldsymbol{\alpha}, \boldsymbol{d}, \boldsymbol{\vartheta}). \tag{2.84}$$

The manipulator's end-effector pose should be measured with high precision for the effectiveness of the kinematic calibration procedure. To this purpose a mechanical apparatus can be used that allows the end-effector to be constrained at given poses with a priori known precision. Alternatively, direct measurement systems of object position and orientation in the Cartesian space can be used which employ triangulation techniques.

Let $\boldsymbol{x}_m$ be the measured pose and $\boldsymbol{x}_n$ the nominal pose that can be computed via (2.84) with the nominal values of the parameters $\boldsymbol{a}$, $\boldsymbol{\alpha}$, $\boldsymbol{d}$, $\boldsymbol{\vartheta}$. The nominal values of the fixed parameters are set equal to the design data of the mechanical structure, whereas the nominal values of the joint variables are set equal to the data provided by the position transducers at the given manipulator posture. The deviation $\Delta\boldsymbol{x} = \boldsymbol{x}_m - \boldsymbol{x}_n$ gives a measure of accuracy at the given posture. On the assumption of small deviations, at first approximation, it is possible to derive the following relation from (2.84):

$$\Delta\boldsymbol{x} = \frac{\partial \boldsymbol{k}}{\partial \boldsymbol{a}}\Delta\boldsymbol{a} + \frac{\partial \boldsymbol{k}}{\partial \boldsymbol{\alpha}}\Delta\boldsymbol{\alpha} + \frac{\partial \boldsymbol{k}}{\partial \boldsymbol{d}}\Delta\boldsymbol{d} + \frac{\partial \boldsymbol{k}}{\partial \boldsymbol{\vartheta}}\Delta\boldsymbol{\vartheta} \tag{2.85}$$

where $\Delta\boldsymbol{a}$, $\Delta\boldsymbol{\alpha}$, $\Delta\boldsymbol{d}$, $\Delta\boldsymbol{\vartheta}$ denote the deviations between the values of the parameters of the real structure and the nominal ones. Moreover, $\partial\boldsymbol{k}/\partial\boldsymbol{a}$, $\partial\boldsymbol{k}/\partial\boldsymbol{\alpha}$, $\partial\boldsymbol{k}/\partial\boldsymbol{d}$, $\partial\boldsymbol{k}/\partial\boldsymbol{\vartheta}$ denote the $(m \times n)$ matrices whose elements are the partial derivatives of the components of the direct kinematics function with respect to the single parameters.[13]

Group the parameters in the $(4n \times 1)$ vector $\boldsymbol{\zeta} = [\,\boldsymbol{a}^T \quad \boldsymbol{\alpha}^T \quad \boldsymbol{d}^T \quad \boldsymbol{\vartheta}^T\,]^T$. Let $\Delta\boldsymbol{\zeta} = \boldsymbol{\zeta}_m - \boldsymbol{\zeta}_n$ denote the parameter variations with respect to the nominal values, and $\boldsymbol{\Phi} = [\,\partial\boldsymbol{k}/\partial\boldsymbol{a} \quad \partial\boldsymbol{k}/\partial\boldsymbol{\alpha} \quad \partial\boldsymbol{k}/\partial\boldsymbol{d} \quad \partial\boldsymbol{k}/\partial\boldsymbol{\vartheta}\,]$ the $(m \times 4n)$ *kinematic calibration matrix* computed for the nominal values of the parameters $\boldsymbol{\zeta}_n$. Then (2.85) can be compactly rewritten as

$$\Delta\boldsymbol{x} = \boldsymbol{\Phi}(\boldsymbol{\zeta}_n)\Delta\boldsymbol{\zeta}. \tag{2.86}$$

It is desired to compute $\Delta\boldsymbol{\zeta}$ starting from the knowledge of $\boldsymbol{\zeta}_n, \boldsymbol{x}_n$ and the measurement of $\boldsymbol{x}_m$. Since (2.86) constitutes a system of m equations into $4n$ unknowns with $m < 4n$, a sufficient number of end-effector pose measurements has to be performed so as to obtain a system of at least $4n$ equations. Therefore, if measurements are made for a number of l poses, (2.86) yields

$$\Delta\bar{\boldsymbol{x}} = \begin{bmatrix} \Delta\boldsymbol{x}_1 \\ \vdots \\ \Delta\boldsymbol{x}_l \end{bmatrix} = \begin{bmatrix} \boldsymbol{\Phi}_1 \\ \vdots \\ \boldsymbol{\Phi}_l \end{bmatrix} \Delta\boldsymbol{\zeta} = \bar{\boldsymbol{\Phi}}\Delta\boldsymbol{\zeta}. \tag{2.87}$$

[13] These matrices are the Jacobians of the transformations between the parameter space and the operational space.

As regards the nominal values of the parameters needed for the computation of the matrices $\boldsymbol{\Phi}_i$, it should be observed that the geometric parameters are constant whereas the joint variables depend on the manipulator configuration at pose i.

In order to avoid ill-conditioning of matrix $\bar{\boldsymbol{\Phi}}$, it is advisable to choose l so that $lm \gg 4n$ and then solve (2.87) with a least-squares technique; in this case the solution is of the form

$$\Delta\boldsymbol{\zeta} = (\bar{\boldsymbol{\Phi}}^T\bar{\boldsymbol{\Phi}})^{-1}\bar{\boldsymbol{\Phi}}^T\Delta\bar{\boldsymbol{x}} \tag{2.88}$$

where $(\bar{\boldsymbol{\Phi}}^T\bar{\boldsymbol{\Phi}})^{-1}\bar{\boldsymbol{\Phi}}^T$ is the *left pseudo-inverse* matrix of $\bar{\boldsymbol{\Phi}}$.[14] By computing $\bar{\boldsymbol{\Phi}}$ with the nominal values of the parameters $\boldsymbol{\zeta}_n$, the first parameter *estimate* is given by

$$\boldsymbol{\zeta}' = \boldsymbol{\zeta}_n + \Delta\boldsymbol{\zeta}. \tag{2.89}$$

This is a nonlinear parameter estimate problem and, as such, the procedure should be iterated until $\Delta\boldsymbol{\zeta}$ converges within a given threshold. At each iteration, the calibration matrix $\bar{\boldsymbol{\Phi}}$ is to be updated with the parameter estimates $\boldsymbol{\zeta}'$ obtained via (2.89) at the previous iteration. In a similar manner, the deviation $\Delta\bar{\boldsymbol{x}}$ is to be computed as the difference between the measured values for the l end-effector poses and the corresponding poses computed by the direct kinematics function with the values of the parameters at the previous iteration. As a result of the kinematic calibration procedure, more accurate estimates of the real manipulator geometric parameters as well as possible corrections to make on the joint transducers measurements are obtained.

Kinematic calibration is an operation that is performed by the robot manufacturer to guarantee the accuracy reported in the data sheet. There is another kind of calibration that is performed by the robot user which is needed for the measurement system *start-up* to guarantee that the position transducers data are consistent with the attained manipulator posture. For instance, in the case of incremental (nonabsolute) position transducers, such calibration consists of taking the mechanical structure into a given reference posture (*home*) and initializing the position transducers with the values at that posture.

2.12 Inverse Kinematics Problem

The direct kinematics equation, either in the form (2.50) or in the form (2.82), establishes the functional relationship between the joint variables and the end-effector position and orientation. The *inverse kinematics problem* consists of the determination of the joint variables corresponding to a given end-effector position and orientation. The solution to this problem is of fundamental importance in order to transform the motion specifications, assigned to the end-effector in the operational space, into the corresponding joint space motions that allow execution of the desired motion.

[14] See Sect. A.7 for the definition of the pseudo-inverse of a matrix.

As regards the direct kinematics equation in (2.50), the end-effector position and rotation matrix are computed in a unique manner, once the joint variables are known[15]. On the other hand, the inverse kinematics problem is much more complex for the following reasons:

- The equations to solve are in general nonlinear, and thus it is not always possible to find a *closed-form solution*.
- *Multiple solutions* may exist.
- *Infinite solutions* may exist, e.g., in the case of a kinematically redundant manipulator.
- There might be no *admissible* solutions, in view of the manipulator kinematic structure.

The existence of solutions is guaranteed only if the given end-effector position and orientation belong to the manipulator dexterous workspace.

On the other hand, the problem of multiple solutions depends not only on the number of DOFs but also on the number of non-null DH parameters; in general, the greater the number of non-null parameters, the greater the number of admissible solutions. For a six-DOF manipulator without mechanical joint limits, there are in general up to 16 admissible solutions. Such occurrence demands some criterion to choose among admissible solutions (e.g., the elbow-up/elbow-down case of Example 2.6). The existence of mechanical joint limits may eventually reduce the number of admissible multiple solutions for the real structure.

Computation of closed-form solutions requires either *algebraic intuition* to find those significant equations containing the unknowns or *geometric intuition* to find those significant points on the structure with respect to which it is convenient to express position and/or orientation as a function of a reduced number of unknowns. The following examples will point out the ability required to an inverse kinematics problem solver. On the other hand, in all those cases when there are no — or it is difficult to find — closed-form solutions, it might be appropriate to resort to *numerical solution techniques*; these clearly have the advantage of being applicable to any kinematic structure, but in general they do not allow computation of all admissible solutions. In the following chapter, it will be shown how suitable algorithms utilizing the manipulator Jacobian can be employed to solve the inverse kinematics problem.

2.12.1 Solution of Three-link Planar Arm

Consider the arm shown in Fig. 2.20 whose direct kinematics was given in (2.63). It is desired to find the joint variables ϑ_1, ϑ_2, ϑ_3 corresponding to a given end-effector position and orientation.

[15] In general, this cannot be said for (2.82) too, since the Euler angles are not uniquely defined.

As already pointed out, it is convenient to specify position and orientation in terms of a minimal number of parameters: the two coordinates p_x, p_y and the angle ϕ with axis x_0, in this case. Hence, it is possible to refer to the direct kinematics equation in the form (2.83).

A first *algebraic solution* technique is illustrated below. Having specified the orientation, the relation

$$\phi = \vartheta_1 + \vartheta_2 + \vartheta_3 \tag{2.90}$$

is one of the equations of the system to solve[16]. From (2.63) the following equations can be obtained:

$$p_{Wx} = p_x - a_3 c_\phi = a_1 c_1 + a_2 c_{12} \tag{2.91}$$

$$p_{Wy} = p_y - a_3 s_\phi = a_1 s_1 + a_2 s_{12} \tag{2.92}$$

which describe the position of point W, i.e., the origin of Frame 2; this depends only on the first two angles ϑ_1 and ϑ_2. Squaring and summing (2.91), (2.92) yields

$$p_{Wx}^2 + p_{Wy}^2 = a_1^2 + a_2^2 + 2a_1 a_2 c_2$$

from which

$$c_2 = \frac{p_{Wx}^2 + p_{Wy}^2 - a_1^2 - a_2^2}{2a_1 a_2}.$$

The existence of a solution obviously imposes that $-1 \leq c_2 \leq 1$, otherwise the given point would be outside the arm reachable workspace. Then, set

$$s_2 = \pm\sqrt{1 - c_2^2},$$

where the positive sign is relative to the elbow-down posture and the negative sign to the elbow-up posture. Hence, the angle ϑ_2 can be computed as

$$\vartheta_2 = \text{Atan2}(s_2, c_2).$$

Having determined ϑ_2, the angle ϑ_1 can be found as follows. Substituting ϑ_2 into (2.91), (2.92) yields an algebraic system of two equations in the two unknowns s_1 and c_1, whose solution is

$$s_1 = \frac{(a_1 + a_2 c_2) p_{Wy} - a_2 s_2 p_{Wx}}{p_{Wx}^2 + p_{Wy}^2}$$

$$c_1 = \frac{(a_1 + a_2 c_2) p_{Wx} + a_2 s_2 p_{Wy}}{p_{Wx}^2 + p_{Wy}^2}.$$

In analogy to the above, it is

$$\vartheta_1 = \text{Atan2}(s_1, c_1).$$

[16] If ϕ is not specified, then the arm is redundant and there exist infinite solutions to the inverse kinematics problem.

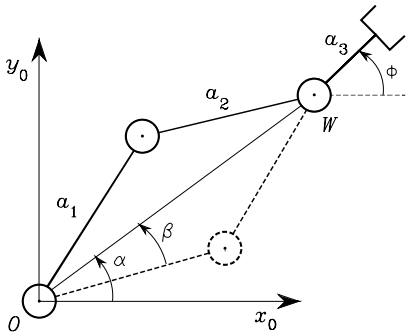

Fig. 2.31. Admissible postures for a two-link planar arm

In the case when $s_2 = 0$, it is obviously $\vartheta_2 = 0, \pi$; as will be shown in the following, in such a posture the manipulator is at a kinematic *singularity*. Yet, the angle ϑ_1 can be determined uniquely, unless $a_1 = a_2$ and it is required $p_{Wx} = p_{Wy} = 0$.

Finally, the angle ϑ_3 is found from (2.90) as

$$\vartheta_3 = \phi - \vartheta_1 - \vartheta_2.$$

An alternative *geometric solution* technique is presented below. As above, the orientation angle is given as in (2.90) and the coordinates of the origin of Frame 2 are computed as in (2.91), (2.92). The application of the cosine theorem to the triangle formed by links a_1, a_2 and the segment connecting points W and O gives

$$p_{Wx}^2 + p_{Wy}^2 = a_1^2 + a_2^2 - 2a_1 a_2 \cos(\pi - \vartheta_2);$$

the two admissible configurations of the triangle are shown in Fig. 2.31. Observing that $\cos(\pi - \vartheta_2) = -\cos\vartheta_2$ leads to

$$c_2 = \frac{p_{Wx}^2 + p_{Wy}^2 - a_1^2 - a_2^2}{2a_1 a_2}.$$

For the existence of the triangle, it must be $\sqrt{p_{Wx}^2 + p_{Wy}^2} \leq a_1 + a_2$. This condition is not satisfied when the given point is outside the arm reachable workspace. Then, under the assumption of admissible solutions, it is

$$\vartheta_2 = \pm\cos^{-1}(c_2);$$

the elbow-up posture is obtained for $\vartheta_2 \in (-\pi, 0)$ while the elbow-down posture is obtained for $\vartheta_2 \in (0, \pi)$.

To find ϑ_1 consider the angles α and β in Fig. 2.31. Notice that the determination of α depends on the sign of p_{Wx} and p_{Wy}; then, it is necessary to compute α as

$$\alpha = \text{Atan2}(p_{Wy}, p_{Wx}).$$

To compute β, applying again the cosine theorem yields

$$c_\beta \sqrt{p_{Wx}^2 + p_{Wy}^2} = a_1 + a_2 c_2$$

and resorting to the expression of c_2 given above leads to

$$\beta = \cos^{-1}\left(\frac{p_{Wx}^2 + p_{Wy}^2 + a_1^2 - a_2^2}{2a_1\sqrt{p_{Wx}^2 + p_{Wy}^2}}\right)$$

with $\beta \in (0, \pi)$ so as to preserve the existence of triangles. Then, it is

$$\vartheta_1 = \alpha \pm \beta,$$

where the positive sign holds for $\vartheta_2 < 0$ and the negative sign for $\vartheta_2 > 0$. Finally, ϑ_3 is computed from (2.90).

It is worth noticing that, in view of the substantial equivalence between the two-link planar arm and the parallelogram arm, the above techniques can be formally applied to solve the inverse kinematics of the arm in Sect. 2.9.2.

2.12.2 Solution of Manipulators with Spherical Wrist

Most of the existing manipulators are kinematically simple, since they are typically formed by an arm, of the kind presented above, and a spherical wrist; see the manipulators in Sects. 2.9.6–2.9.8. This choice is partly motivated by the difficulty to find solutions to the inverse kinematics problem in the general case. In particular, a *six*-DOF kinematic structure has closed-form inverse kinematics solutions if:

- three consecutive revolute joint axes intersect at a common point, like for the spherical wrist;
- three consecutive revolute joint axes are parallel.

In any case, algebraic or geometric intuition is required to obtain closed-form solutions.

Inspired by the previous solution to a three-link planar arm, a suitable point along the structure can be found whose position can be expressed both as a function of the given end-effector position and orientation and as a function of a reduced number of joint variables. This is equivalent to articulating the inverse kinematics problem into two subproblems, since the solution for the *position* is *decoupled* from that for the *orientation*.

For a manipulator with spherical wrist, the natural choice is to locate such point W at the intersection of the three terminal revolute axes (Fig. 2.32). In fact, once the end-effector position and orientation are specified in terms of $\boldsymbol{p}_e$ and $\boldsymbol{R}_e = [\,\boldsymbol{n}_e \quad \boldsymbol{s}_e \quad \boldsymbol{a}_e\,]$, the wrist position can be found as

$$\boldsymbol{p}_W = \boldsymbol{p}_e - d_6 \boldsymbol{a}_e \tag{2.93}$$

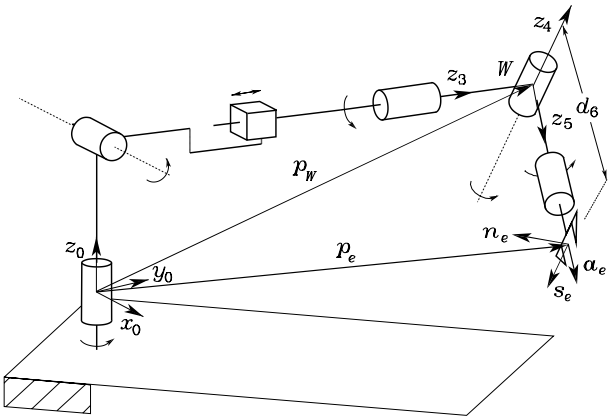

Fig. 2.32. Manipulator with spherical wrist

which is a function of the sole joint variables that determine the arm position[17]. Hence, in the case of a (nonredundant) three-DOF arm, the inverse kinematics can be solved according to the following steps:

- Compute the wrist position $\boldsymbol{p}_W(q_1, q_2, q_3)$ as in (2.93).
- Solve inverse kinematics for (q_1, q_2, q_3).
- Compute $\boldsymbol{R}_3^0(q_1, q_2, q_3)$.
- Compute $\boldsymbol{R}_6^3(\vartheta_4, \vartheta_5, \vartheta_6) = \boldsymbol{R}_3^{0T}\boldsymbol{R}$.
- Solve inverse kinematics for orientation $(\vartheta_4, \vartheta_5, \vartheta_6)$.

Therefore, on the basis of this kinematic decoupling, it is possible to solve the inverse kinematics for the arm separately from the inverse kinematics for the spherical wrist. Below are presented the solutions for two typical arms (spherical and anthropomorphic) as well as the solution for the spherical wrist.

2.12.3 Solution of Spherical Arm

Consider the spherical arm shown in Fig. 2.22, whose direct kinematics was given in (2.65). It is desired to find the joint variables ϑ_1, ϑ_2, d_3 corresponding to a given end-effector position $\boldsymbol{p}_W$.

In order to separate the variables on which $\boldsymbol{p}_W$ depends, it is convenient to express the position of $\boldsymbol{p}_W$ with respect to Frame 1; then, consider the matrix equation

$$(\boldsymbol{A}_1^0)^{-1}\boldsymbol{T}_3^0 = \boldsymbol{A}_2^1\boldsymbol{A}_3^2.$$

[17] Note that the same reasoning was implicitly adopted in Sect. 2.12.1 for the three-link planar arm; $\boldsymbol{p}_W$ described the one-DOF wrist position for the two-DOF arm obtained by considering only the first two links.

Equating the first three elements of the fourth columns of the matrices on both sides yields

$$\boldsymbol{p}_W^1 = \begin{bmatrix} p_{Wx}c_1 + p_{Wy}s_1 \\ -p_{Wz} \\ -p_{Wx}s_1 + p_{Wy}c_1 \end{bmatrix} = \begin{bmatrix} d_3 s_2 \\ -d_3 c_2 \\ d_2 \end{bmatrix} \tag{2.94}$$

which depends only on ϑ_2 and d_3. To solve this equation, set

$$t = \tan \frac{\vartheta_1}{2}$$

so that

$$c_1 = \frac{1 - t^2}{1 + t^2} \qquad s_1 = \frac{2t}{1 + t^2}.$$

Substituting this equation in the third component on the left-hand side of (2.94) gives

$$(d_2 + p_{Wy})t^2 + 2p_{Wx}t + d_2 - p_{Wy} = 0,$$

whose solution is

$$t = \frac{-p_{Wx} \pm \sqrt{p_{Wx}^2 + p_{Wy}^2 - d_2^2}}{d_2 + p_{Wy}}.$$

The two solutions correspond to two different postures. Hence, it is

$$\vartheta_1 = 2\text{Atan2}\left(-p_{Wx} \pm \sqrt{p_{Wx}^2 + p_{Wy}^2 - d_2^2},\ d_2 + p_{Wy}\right).$$

Once ϑ_1 is known, squaring and summing the first two components of (2.94) yields

$$d_3 = \sqrt{(p_{Wx}c_1 + p_{Wy}s_1)^2 + p_{Wz}^2},$$

where only the solution with $d_3 \geq 0$ has been considered. Note that the same value of d_3 corresponds to both solutions for ϑ_1. Finally, if $d_3 \neq 0$, from the first two components of (2.94) it is

$$\frac{p_{Wx}c_1 + p_{Wy}s_1}{-p_{Wz}} = \frac{d_3 s_2}{-d_3 c_2},$$

from which

$$\vartheta_2 = \text{Atan2}(p_{Wx}c_1 + p_{Wy}s_1, p_{Wz}).$$

Notice that, if $d_3 = 0$, then ϑ_2 cannot be uniquely determined.

2.12.4 Solution of Anthropomorphic Arm

Consider the anthropomorphic arm shown in Fig. 2.23. It is desired to find the joint variables ϑ_1, ϑ_2, ϑ_3 corresponding to a given end-effector position $\boldsymbol{p}_W$. Notice that the direct kinematics for $\boldsymbol{p}_W$ is expressed by (2.66) which can

be obtained from (2.70) by setting $d_6 = 0$, $d_4 = a_3$ and replacing ϑ_3 with the angle $\vartheta_3 + \pi/2$ because of the misalignment of the Frames 3 for the structures in Fig. 2.23 and in Fig. 2.26, respectively. Hence, it follows

$$p_{Wx} = c_1(a_2c_2 + a_3c_{23}) \tag{2.95}$$
$$p_{Wy} = s_1(a_2c_2 + a_3c_{23}) \tag{2.96}$$
$$p_{Wz} = a_2s_2 + a_3s_{23}. \tag{2.97}$$

Proceeding as in the case of the two-link planar arm, it is worth squaring and summing (2.95)–(2.97) yielding

$$p_{Wx}^2 + p_{Wy}^2 + p_{Wz}^2 = a_2^2 + a_3^2 + 2a_2a_3c_3$$

from which

$$c_3 = \frac{p_{Wx}^2 + p_{Wy}^2 + p_{Wz}^2 - a_2^2 - a_3^2}{2a_2a_3} \tag{2.98}$$

where the admissibility of the solution obviously requires that $-1 \leq c_3 \leq 1$, or equivalently $|a_2 - a_3| \leq \sqrt{p_{Wx}^2 + p_{Wy}^2 + p_{Wz}^2} \leq a_2 + a_3$, otherwise the wrist point is outside the reachable workspace of the manipulator. Hence it is

$$s_3 = \pm\sqrt{1 - c_3^2} \tag{2.99}$$

and thus

$$\vartheta_3 = \text{Atan2}(s_3, c_3)$$

giving the two solutions, according to the sign of s_3,

$$\vartheta_{3,\text{I}} \in [-\pi, \pi] \tag{2.100}$$
$$\vartheta_{3,\text{II}} = -\vartheta_{3,I}. \tag{2.101}$$

Having determined ϑ_3, it is possible to compute ϑ_2 as follows. Squaring and summing (2.95), (2.96) gives

$$p_{Wx}^2 + p_{Wy}^2 = (a_2c_2 + a_3c_{23})^2$$

from which

$$a_2c_2 + a_3c_{23} = \pm\sqrt{p_{Wx}^2 + p_{Wy}^2}. \tag{2.102}$$

The system of the two Eqs. (2.102), (2.97), for each of the solutions (2.100), (2.101), admits the solutions:

$$c_2 = \frac{\pm\sqrt{p_{Wx}^2 + p_{Wy}^2}(a_2 + a_3c_3) + p_{Wz}a_3s_3}{a_2^2 + a_3^2 + 2a_2a_3c_3} \tag{2.103}$$

$$s_2 = \frac{p_{Wz}(a_2 + a_3c_3) \mp \sqrt{p_{Wx}^2 + p_{Wy}^2}a_3s_3}{a_2^2 + a_3^2 + 2a_2a_3c_3}. \tag{2.104}$$

From (2.103), (2.104) it follows

$$\vartheta_2 = \text{Atan2}(s_2, c_2)$$

which gives the four solutions for ϑ_2, according to the sign of s_3 in (2.99):

$$\vartheta_{2,\text{I}} = \text{Atan2}\left((a_2 + a_3 c_3)p_{Wz} - a_3 s_3^+ \sqrt{p_{Wx}^2 + p_{Wy}^2},\right.$$
$$\left.(a_2 + a_3 c_3)\sqrt{p_{Wx}^2 + p_{Wy}^2} + a_3 s_3^+ p_{Wz}\right) \tag{2.105}$$

$$\vartheta_{2,\text{II}} = \text{Atan2}\left((a_2 + a_3 c_3)p_{Wz} + a_3 s_3^+ \sqrt{p_{Wx}^2 + p_{Wy}^2},\right.$$
$$\left.-(a_2 + a_3 c_3)\sqrt{p_{Wx}^2 + p_{Wy}^2} + a_3 s_3^+ p_{Wz}\right) \tag{2.106}$$

corresponding to $s_3^+ = \sqrt{1 - c_3^2}$, and

$$\vartheta_{2,\text{III}} = \text{Atan2}\left((a_2 + a_3 c_3)p_{Wz} - a_3 s_3^- \sqrt{p_{Wx}^2 + p_{Wy}^2},\right.$$
$$\left.(a_2 + a_3 c_3)\sqrt{p_{Wx}^2 + p_{Wy}^2} + a_3 s_3^- p_{Wz}\right) \tag{2.107}$$

$$\vartheta_{2,\text{IV}} = \text{Atan2}\left((a_2 + a_3 c_3)p_{Wz} + a_3 s_3^- \sqrt{p_{Wx}^2 + p_{Wy}^2},\right.$$
$$\left.-(a_2 + a_3 c_3)\sqrt{p_{Wx}^2 + p_{Wy}^2} + a_3 s_3^- p_{Wz}\right) \tag{2.108}$$

corresponding to $s_3^- = -\sqrt{1 - c_3^2}$.

Finally, to compute ϑ_1, it is sufficient to rewrite (2.95), (2.96), using (2.102), as

$$p_{Wx} = \pm c_1 \sqrt{p_{Wx}^2 + p_{Wy}^2}$$
$$p_{Wy} = \pm s_1 \sqrt{p_{Wx}^2 + p_{Wy}^2}$$

which, once solved, gives the two solutions:

$$\vartheta_{1,\text{I}} = \text{Atan2}(p_{Wy}, p_{Wx}) \tag{2.109}$$
$$\vartheta_{1,\text{II}} = \text{Atan2}(-p_{Wy}, -p_{Wx}). \tag{2.110}$$

Notice that (2.110) gives[18]

$$\vartheta_{1,\text{II}} = \begin{cases} \text{Atan2}(p_{Wy}, p_{Wx}) - \pi & p_{Wy} \geq 0 \\ \text{Atan2}(p_{Wy}, p_{Wx}) + \pi & p_{Wy} < 0. \end{cases}$$

[18] It is easy to show that $\text{Atan2}(-y, -x) = -\text{Atan2}(y, -x)$ and

$$\text{Atan2}(y, -x) = \begin{cases} \pi - \text{Atan2}(y, x) & y \geq 0 \\ -\pi - \text{Atan2}(y, x) & y < 0. \end{cases}$$

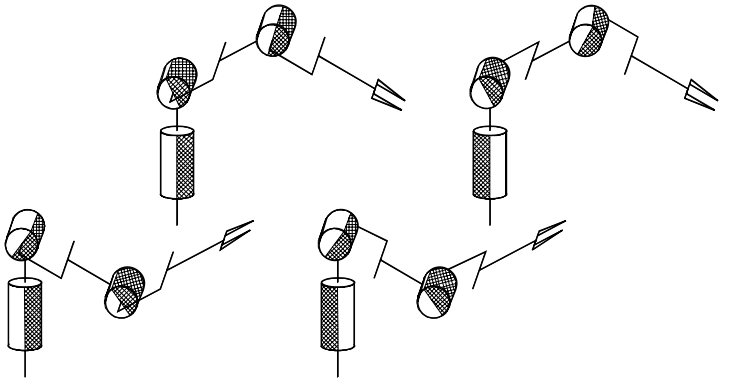

Fig. 2.33. The four configurations of an anthropomorphic arm compatible with a given wrist position

As can be recognized, there exist four solutions according to the values of ϑ_3 in (2.100), (2.101), ϑ_2 in (2.105)–(2.108) and ϑ_1 in (2.109), (2.110):

$$(\vartheta_{1,\mathrm{I}}, \vartheta_{2,\mathrm{I}}, \vartheta_{3,\mathrm{I}}) \quad (\vartheta_{1,\mathrm{I}}, \vartheta_{2,\mathrm{III}}, \vartheta_{3,\mathrm{II}}) \quad (\vartheta_{1,\mathrm{II}}, \vartheta_{2,\mathrm{II}}, \vartheta_{3,\mathrm{I}}) \quad (\vartheta_{1,\mathrm{II}}, \vartheta_{2,\mathrm{IV}}, \vartheta_{3,\mathrm{II}}),$$

which are illustrated in Fig. 2.33: shoulder–right/elbow–up, shoulder–left/elbow–up, shoulder–right/elbow–down, shoulder–left/elbow–down; obviously, the forearm orientation is different for the two pairs of solutions.

Notice finally how it is possible to find the solutions only if at least

$$p_{Wx} \neq 0 \qquad \text{or} \qquad p_{Wy} \neq 0.$$

In the case $p_{Wx} = p_{Wy} = 0$, an infinity of solutions is obtained, since it is possible to determine the joint variables ϑ_2 and ϑ_3 independently of the value of ϑ_1; in the following, it will be seen that the arm in such configuration is kinematically *singular* (see Problem 2.18).

2.12.5 Solution of Spherical Wrist

Consider the spherical wrist shown in Fig. 2.24, whose direct kinematics was given in (2.67). It is desired to find the joint variables ϑ_4, ϑ_5, ϑ_6 corresponding to a given end-effector orientation $\boldsymbol{R}_6^3$. As previously pointed out, these angles constitute a set of Euler angles ZYZ with respect to Frame 3. Hence, having computed the rotation matrix

$$\boldsymbol{R}_6^3 = \begin{bmatrix} n_x^3 & s_x^3 & a_x^3 \\ n_y^3 & s_y^3 & a_y^3 \\ n_z^3 & s_z^3 & a_z^3 \end{bmatrix},$$

from its expression in terms of the joint variables in (2.67), it is possible to compute the solutions directly as in (2.19), (2.20), i.e.,

$$\begin{aligned} \vartheta_4 &= \text{Atan2}(a_y^3, a_x^3) \\ \vartheta_5 &= \text{Atan2}\Big(\sqrt{(a_x^3)^2 + (a_y^3)^2}, a_z^3\Big) \\ \vartheta_6 &= \text{Atan2}(s_z^3, -n_z^3) \end{aligned} \tag{2.111}$$

for $\vartheta_5 \in (0, \pi)$, and

$$\begin{aligned} \vartheta_4 &= \text{Atan2}(-a_y^3, -a_x^3) \\ \vartheta_5 &= \text{Atan2}\Big(-\sqrt{(a_x^3)^2 + (a_y^3)^2}, a_z^3\Big) \\ \vartheta_6 &= \text{Atan2}(-s_z^3, n_z^3) \end{aligned} \tag{2.112}$$

for $\vartheta_5 \in (-\pi, 0)$.

Bibliography

The treatment of kinematics of robot manipulators can be found in several classical robotics texts, such as [180, 10, 200, 217]. Specific texts are [23, 6, 151].

For the descriptions of the orientation of a rigid body, see [187]. Quaternion algebra can be found in [46]; see [204] for the extraction of quaternions from rotation matrices.

The Denavit–Hartenberg convention was first introduced in [60]. A modified version is utilized in [53, 248, 111]. The use of homogeneous transformation matrices for the computation of open-chain manipulator direct kinematics is presented in [181], while in [183] sufficient conditions are given for the closed-form computation of the inverse kinematics problem. For kinematics of closed chains see [144, 111]. The design of the Stanford manipulator is due to [196].

The problem of kinematic calibration is considered in [188, 98]. Methods which do not require the use of external sensors for direct measurement of end-effector position and orientation are proposed in [68].

The kinematic decoupling deriving from the spherical wrist is utilized in [76, 99, 182]. Numerical methods for the solution of the inverse kinematics problem based on iterative algorithms are proposed in [232, 86].

Problems

2.1. Find the rotation matrix corresponding to the set of Euler angles ZXZ.

2.2. Discuss the inverse solution for the Euler angles ZYZ in the case $s_\vartheta = 0$.

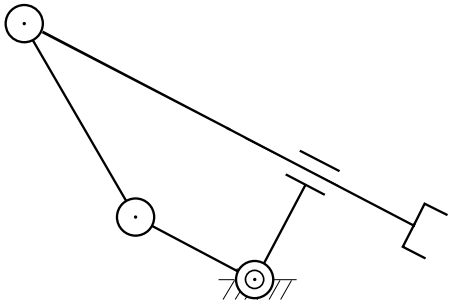

Fig. 2.34. Four-link closed-chain planar arm with prismatic joint

2.3. Discuss the inverse solution for the Roll–Pitch–Yaw angles in the case $c_\vartheta = 0$.

2.4. Verify that the rotation matrix corresponding to the rotation by an angle about an arbitrary axis is given by (2.25).

2.5. Prove that the angle and the unit vector of the axis corresponding to a rotation matrix are given by (2.27), (2.28). Find inverse formulae in the case of $\sin\vartheta = 0$.

2.6. Verify that the rotation matrix corresponding to the unit quaternion is given by (2.33).

2.7. Prove that the unit quaternion is invariant with respect to the rotation matrix and its transpose, i.e., $\boldsymbol{R}(\eta, \boldsymbol{\epsilon})\boldsymbol{\epsilon} = \boldsymbol{R}^T(\eta, \boldsymbol{\epsilon})\boldsymbol{\epsilon} = \boldsymbol{\epsilon}$.

2.8. Prove that the unit quaternion corresponding to a rotation matrix is given by (2.34), (2.35).

2.9. Prove that the quaternion product is expressed by (2.37).

2.10. By applying the rules for inverting a block-partitioned matrix, prove that matrix $\boldsymbol{A}_0^1$ is given by (2.45).

2.11. Find the direct kinematics equation of the four-link closed-chain planar arm in Fig. 2.34, where the two links connected by the prismatic joint are orthogonal to each other.

2.12. Find the direct kinematics equation for the cylindrical arm in Fig. 2.35.

2.13. Find the direct kinematics equation for the SCARA manipulator in Fig. 2.36.

2.14. Find the complete direct kinematics equation for the humanoid manipulator in Fig. 2.28.

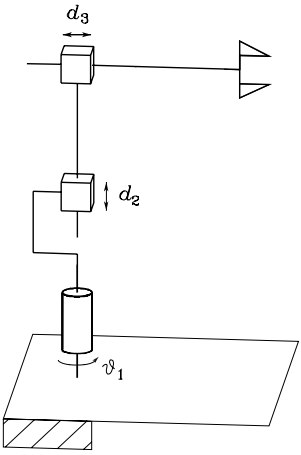

Fig. 2.35. Cylindrical arm

2.15. For the set of minimal representations of orientation $\boldsymbol{\phi}$, define the sum operation in terms of the composition of rotations. By means of an example, show that the commutative property does not hold for that operation.

2.16. Consider the elementary rotations about coordinate axes given by infinitesimal angles. Show that the rotation resulting from any two elementary rotations does not depend on the order of rotations. [*Hint*: for an infinitesimal angle $d\phi$, approximate $\cos(d\phi) \approx 1$ and $\sin(d\phi) \approx d\phi \ldots$]. Further, define $\boldsymbol{R}(d\phi_x, d\phi_y, d\phi_z) = \boldsymbol{R}_x(d\phi_x)\boldsymbol{R}_y(d\phi_y)\boldsymbol{R}_z(d\phi_z)$; show that

$$\boldsymbol{R}(d\phi_x, d\phi_y, d\phi_z)\boldsymbol{R}(d\phi'_x, d\phi'_y, d\phi'_z) = \boldsymbol{R}(d\phi_x + d\phi'_x, d\phi_y + d\phi'_y, d\phi_z + d\phi'_z).$$

2.17. Draw the workspace of the three-link planar arm in Fig. 2.20 with the data:

$$a_1 = 0.5 \qquad a_2 = 0.3 \qquad a_3 = 0.2$$

$$-\pi/3 \leq q_1 \leq \pi/3 \qquad -2\pi/3 \leq q_2 \leq 2\pi/3 \qquad -\pi/2 \leq q_3 \leq \pi/2.$$

2.18. With reference to the inverse kinematics of the anthropomorphic arm in Sect. 2.12.4, discuss the number of solutions in the singular cases of $s_3 = 0$ and $p_{Wx} = p_{Wy} = 0$.

2.19. Solve the inverse kinematics for the cylindrical arm in Fig. 2.35.

2.20. Solve the inverse kinematics for the SCARA manipulator in Fig. 2.36.

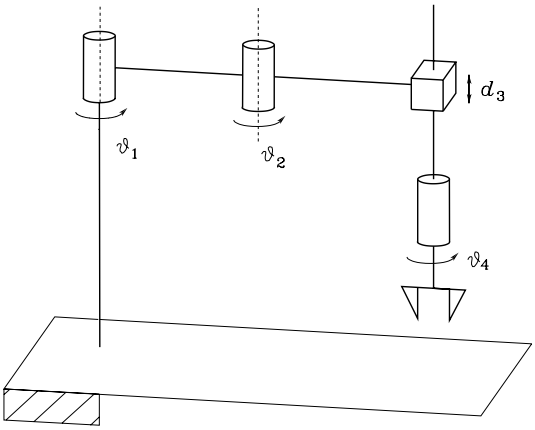

Fig. 2.36. SCARA manipulator